On the Mound of *Macrotermes michaelseni* as an Organ of Respiratory Gas Exchange

J. Scott Turner*

Department of Environmental and Forest Biology, College of Environmental Science and Forestry, State University of New York, Syracuse, New York 13210

ABSTRACT

Patterns and rates of air movements in the mounds and nests of *Macrotermes michaelseni* were studied using tracer methods. Wind is a significant source of energy for powering nest ventilation, despite the mound being a completely enclosed structure. Nests are ventilated by a tidal movement of air driven by temporal variation in wind speed and wind direction. Density gradients sufficiently steep to drive bulk flow by natural convection will be rare. However, metabolism-induced buoyant forces may interact with wind energy in a way that promotes homeostasis of the mound atmosphere.

Introduction

Mounds built by termites of the family Macrotermitinae are a prominent feature of the tropical savannas of southern Africa (Harris 1956; Kalshoven 1956; Lüscher 1961; Ruelle 1964; Ruelle et al. 1975; Pomeroy 1977; Collins 1979; Darlington 1984, 1985). The colony that constructs the mound comprises as many as 2 million individual termites. Surprisingly, the mound is not a habitation but is simply the most visible component of a structure that extends well below the ground. The mound is not a haphazard pile of spoil from excavation of the nest either. Within the mound and surrounding the nest is an extensive and stereotyped network of air spaces (Fig. 1; Darlington 1985; Turner 2000*a*).

The complex architecture of the mound implies some physiological function, and prevailing opinion has long been that the mound functions to regulate the nest environment (Lüscher 1956, 1961; Wilson 1971; Darlington et al. 1997). In the late 1950s, the Swiss entomologist Martin Lüscher proposed that the mound of *Macrotermes bellicosus* (misidentified by Luscher as *Macrotermes natalensis*; Ruelle 1970) functions essentially as a colonial heart-lung machine (Lüscher 1956, 1961). In this conception, the colony's high metabolic rate, which by some estimates runs into the hundreds of watts (Darlington et al. 1997), heats and humidifies the nest air, reducing its density. The resulting buoyant forces circulate air through the nest and the surface tunnels, which are sites for exchange of heat and respiratory gases. Homeostasis of the nest environment follows from a linkage between circulation rate and metabolism. Higher rates of metabolism supposedly impart greater buoyant forces to the nest air, which would in turn drive a more vigorous circulation. This mechanism has been called "thermosiphon ventilation," although a more accurate designation would be "metabolism-induced natural convection."

Lüscher's (1956, 1961) ingenious idea enjoys widespread acceptance today but not because there is positive evidence supporting it. The postulated thermosiphon flows were inferred from distributions of temperature, humidity, and oxygen concentration measured within the mounds, and metabolism-induced natural convection is but one way to explain his results. Consequently, Lüscher's (1956, 1961) thermosiphon model has, since its inception, been criticized for failing to account for the complex variation of mound architecture among the macrotermitines and for the interactions of the mound with wind and other aspects of the physical environment, notably temperature (Loos 1964; Ruelle 1964; Korb and Linsenmaier 2000).

The thermosiphon model makes testable predictions, however, which can be falsified if large-scale patterns and rates of airflow within the mound and nest can be measured. This article reports such measurements in the nests and mounds of *Macrotermes michaelseni*, a widely distributed species that builds enclosed mounds similar to those of *M. natalensis* and *M. bellicosus*. I have found that, while aspects of the thermosiphon model have merit, patterns and rates of airflow and gas exchange in these mounds are far more complex than those predicted by Lüscher. These data clarify how the mounds function as organs of external physiology (sensu Turner 2000*b*) and how social homeostasis emerges from the complex architecture of the mound.

Material and Methods

Species

The subject of this study is the southern African *Macrotermes michaelseni* Sjöstedt, formerly *Macrotermes mossambicus* Holm-

gren (Termitidae, Macrotermitinae; Ruelle 1975). These termites are widely distributed throughout the savanna habitats of sub-Saharan Africa (Grassé and Noirot 1961; Ruelle 1964, 1985; Pomeroy 1977; Abe and Darlington 1985; Turner 2000*a*). Like all macrotermitines, *M. michaelseni* maintains a symbiosis with a fungus, *Termitomyces* spp., that aids in digesting cellulose (Batra and Batra 1979; Garnier-Sillam et al. 1988; Rouland et al. 1991).

I have described the structure of the *M. michaelseni* mound in some detail elsewhere (Turner 2000*a*). However, a few comments about the structure of the mound and nest are necessary here. The workers, reproductives, and fungal symbionts are housed in a nest that occupies a roughly spherical space about 1.5–2.0 m in diameter (Fig. 1). The distribution of biomass in the nest is stratified. The queen, workers, and nursery galleries are contained within the nest proper, while covering the top of the nest is an array of chambers housing fungus combs, the so-called fungus garden. Surrounding the nest is a network of tunnels that extend around and below the nest (Fig. 1). These tunnels merge above the fungus combs to form a central chimney that extends upward into the mound. The chimney itself is at the center of a reticulum of tunnels that extends throughout the mound, termed the "lateral connectives." The lateral connectives merge into a series of vertically oriented surface conduits that underlie roughly 20% of the mound surface. The surface conduits are separated from the outside air by a porous covering that is 1–3 cm thick. The *M. michaelseni* mound is a typical "enclosed" mound (sensu Korb and Linsenmair 2000).
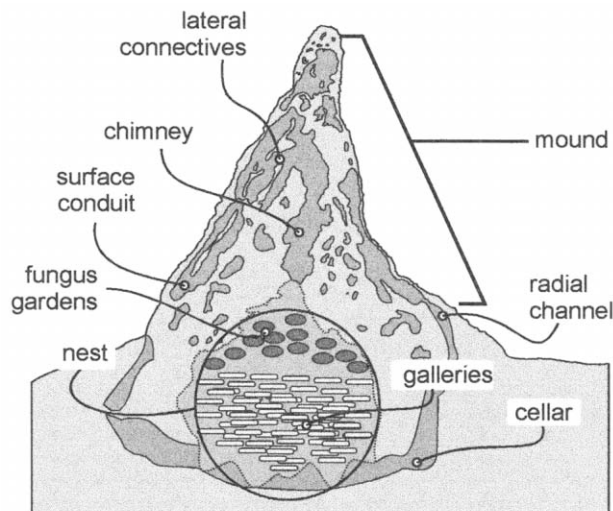

Figure 1. Stylized cross section of the nest and mound of *Macrotermes michaelseni* based upon cross sections of a mound dissected on the Namatubis study site in northern Namibia (Turner 2000*a*).
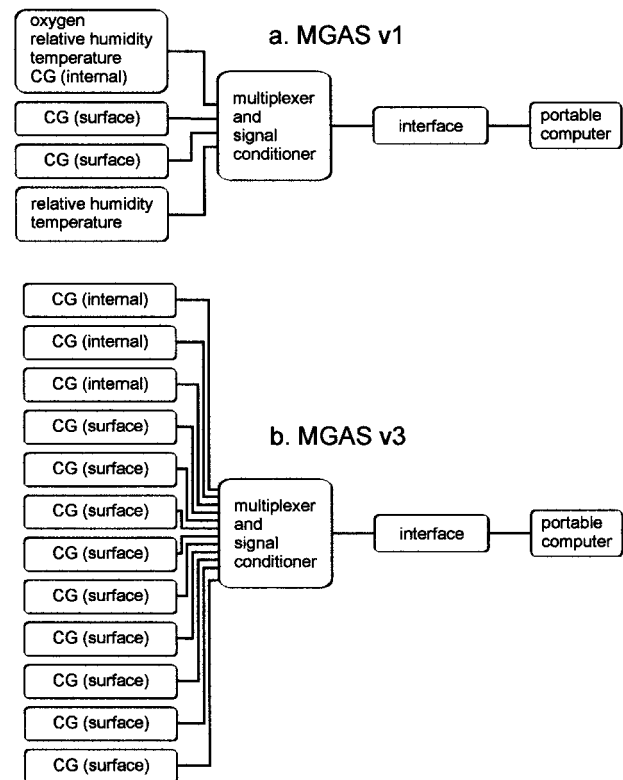

Figure 2. Schematic of the two versions of the mound gas analysis system (MGAS) used in this study. *a*, MGAS version 1, used to measure temperature, oxygen, humidity, and combustible gas concentration (CG) inside and outside the mound and nest. *b*, MGAS version 3, which managed 12 combustible gas sensors. The three sensors designated internal could also be used to measure external or surface CG.

Study Site

The study site was situated in the Republic of Namibia, on the farm Namatubis, 13 km north of Outjo (lat. 16°09′E, long. 20°06′S; elevation 1,330 m). This region is part of the high plateau (1,200–2,000 m) that occupies most of the eastern half of the country. The local topography is flat, interspersed with linear ranges of low hills. The vegetation is classified by Coaton and Sheasby (1972) as mopane savanna, with about 450 mm mean annual rainfall. The work was carried out over six expeditions to the study site from 1995 through 1997: three in the austral winter (July–August) and three in the austral summer (December–January).

Mounds were selected for study along a 2-km stretch of unpaved service road on the farm. Mounds were selected in this way to keep distances for transporting equipment from vehicles to the mound reasonably short. A total of 45 mounds was selected, drawn from a sampled area of about 40 ha. Each mound was permanently marked with metal tags. Basal circumference, mound height, and estimated volume were mea-

sured for each mound according to protocols outlined in Turner (2000*a*).

Tracer Studies

Patterns and rates of movement of gases in the nest and mound were measured using propane as a tracer gas. All tracer experiments used a mound gas analysis system (MGAS), described more fully below.

Rates of air turnover were measured at various locations in the nest and mound. These were quantified using the time constant for clearance, τ (min), of an injected bolus of a 0.01% propane-air mixture. The time constant is the inverse of the more familiar rate constant, k (min^{-1}). It is the time required for the tracer gas concentration in a space to fall to the fraction $1/e$, or ~0.3679 the value of its original concentration. As a rough rule of thumb, 95% of the air in a space will turn over in a period of three time constants.

Patterns of air movements were assessed using pulse-chase experiments. A bolus of a 10% propane-air mixture was injected into a particular site within the mound, designated the injection point. Patterns and speeds of air movement were assessed by detecting and timing the appearance of tracer at various localities in the mound and nest.

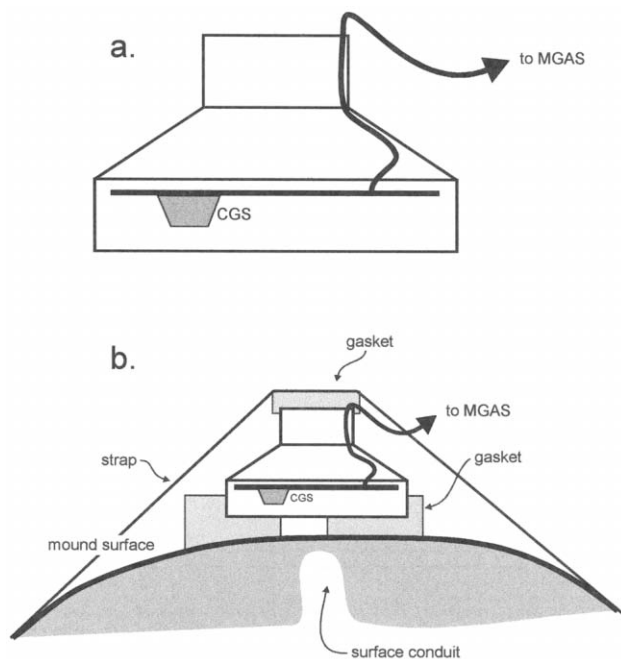Tracers were mixed just before injection using serial dilution

Figure 3. Schematic of the surface sensor carriage. *a*, The sensor carriage with the combustible gas sensor (CGS) mounted in it. *b*, Detail showing attachment of surface sensor to mound surface and placement of gaskets.
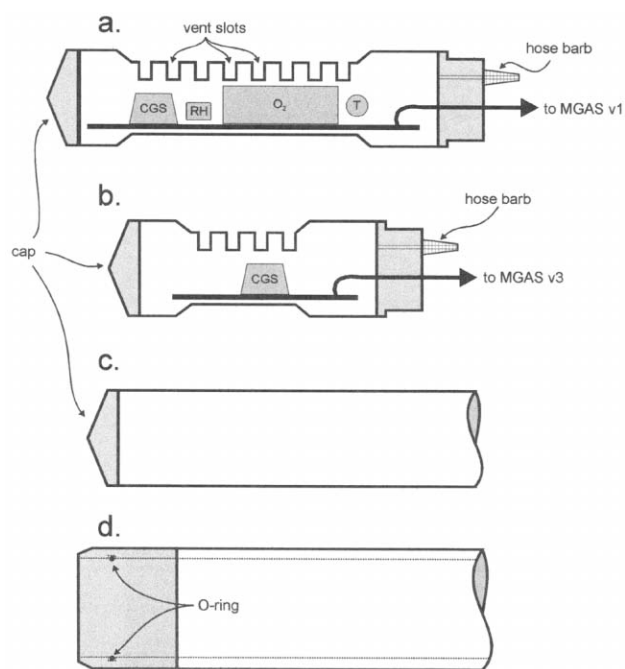
Figure 4. Schematic of the internal sensor carriage for mound gas analysis system (MGAS) version 1 and MGAS version 3 and details of the shaft liner system. *a*, Sensor carriage for MGAS version 1, showing placement of sensors in slotted housing and locations of hose barb for injection of gas and egress of wires for electronics. *b*, Sensor carriage for MGAS version 3. *c*, Sealed plug that sits in the shaft liner before an experiment. *d*, Shaft liner, showing fitting for O-ring that seals around the shaft plug or the sensor carriage.

of 100% propane in a 500-mL graduated syringe. The bolus of tracer was in all cases 500 mL.

Mound Gas Analysis System

Tracer experiments were carried out using two versions of a MGAS that were developed and constructed in my laboratory. The MGAS consists of five components: a sensor array and sensor carriage assembly, a shaft liner and shaft plug system, a multiplexed signal conditioner and power manager for the sensors, an analog/digital and digital/analog converter, and a portable computer (Fig. 2). The components are described in detail below.

Sensory Array and Sensor Carriages. For version 1 of the MGAS, four types of sensors were used (Fig. 2): combustible gas concentration (TGS 813, Figaro Engineering, Skokie, Ill.), P_{O_2} (KD-50, Figaro Engineering), temperature (LM35, National Semiconductor, Santa Clara, Calif.), and humidity (IH 3602-A, Hy-Cal Engineering, El Monte, Calif.). The MGAS version 1 employed three combustible gas sensors (CGS): two for measuring tracer concentrations at the mound surface and a third

Table 1: Temperature, humidity, and oxygen concentration in nests of *Macrotermes michaelseni* in winter and summer

	Winter		Summer		Morning		Afternoon	
	Mean (SD)	n	Mean (SD)	n	Mean (SD)	n	Mean (SD)	n
Temperature (°C):								
Nest	26.19 (4.18)	30	31.73 (2.94)	19	26.67 (4.93)	28	30.56 (3.02)	21
Environment	23.65 (9.86)	30	31.16 (10.97)	19	21.44 (10.94)	28	33.40 (5.88)	21
dT[a]	+2.53 (6.76)	30	+.57 (8.38)	19	+5.23 (7.52)	28	−2.84 (4.03)	21
Humidity (kPa):								
Nest	2.58 (.29)	15	3.40 (.43)	18	2.99 (.50)	20	3.08 (.65)	13
Environment	.35 (.21)	15	.83 (.56)	18	.65 (.51)	20	.55 (.47)	13
dP_{H_2O}[a]	+2.23 (.23)	15	+2.57 (.47)	18	+2.34 (.37)	20	+2.53 (.46)	13
Oxygen (kPa):								
dP_{O_2}[a]	−1.81 (.59)	30	−1.53 (.69)	19	−1.55 (.56)	28	−1.89 (.69)	22
CG	964 (1,322)	11	1,448 (4,111)	11				

Note. Data are reported as mean (SD); n = sample size. CG (combustible gas concentration) is reported in parts per million methane equivalents.

[a] Nest − environment.

for measuring tracer concentrations in the nest or mound interior. Oxygen, temperature, and humidity sensors were mounted with the internal combustible gas sensor on a sensor carriage, described more fully below. Temperature and humidity sensors also measured these properties in the outside air.

Temperature sensors were calibrated against a standard mercury thermometer. Sensors for humidity were calibrated by enclosing them in sealed chambers over saturated solutions of various salts (Tracy et al. 1980). The oxygen sensor was calibrated by enclosing it in a chamber with known mixtures of nitrogen and air. The combustible gas sensors were calibrated by enclosing them in chamber with known mixtures of methane and air. All concentrations of combustible gas are reported as methane equivalents.

The sensors were mounted on one of three types of sensor carriage. Combustible gas sensors for surface measurements were mounted on a printed circuit board fixed in the wide mouth of a 3 × 1 1/2-inch PVC couple (Fig. 3a). The wide end of the couple was also covered with 1-mm aluminum screen to keep termites from the sensors. The surface sensor carriages were affixed tightly to the mound surface using nylon webbing straps, which pressed the wide end of the couple against a foam rubber gasket on the mound surface. The narrow end of the couple was plugged with a foam rubber gasket to eliminate interference from wind (Fig. 3b).

External sensors for temperature and relative humidity were mounted on a sensor carriage similar to the surface CGS carriages described above. During experiments, the external temperature and relative humidity sensors were mounted on a 1.5-m pole in a shady location adjacent to the mound.

The internal sensor carriage for MGAS version 1 carried sensors for combustible gas concentration, oxygen concentration, relative humidity, and temperature (Fig. 4a). Sensors were mounted on a printed circuit board inside a plugged section of 40-mm PVC pipe. The plugged section of the pipe had vent slots to expose the sensors to the nest's internal atmosphere and was covered with 1-mm mesh aluminum screen to exclude termites from the sensors. The plugged pipe, along with the shaft liner system described below, provided a sealed point in the nest or mound interior for placement of the sensors and injection of tracer. The internal sensor carriage for MGAS version 3 was similar, except that it carried only one combustible gas sensor (Fig. 4b). The time constants for clearance of tracer gas from both types of internal sensor carriage was 23–28 s in still room air.

Shaft Liner and Shaft Plug System. A shaft liner/shaft plug system was devised to place internal sensors into the mound and to eliminate leaks between the outside air and the spaces occupied by the internal sensors (Fig. 4c, 4d). The shaft liner was a length of 50-mm PVC pipe, fitted on the end with an internal O-ring

Table 2: Covariation of internal and external temperatures and humidities and the effect of season

Effect	Slope (SD)	r^2 (%)
T_{in} vs. T_{out}:		
All	$T_{in} = 18.86 (.97) + .36 (.03) T_{out}$	70.4
Winter only	$T_{in} = 17.79 (1.12) + .35 (.04) T_{out}$	70.0
Summer only	$T_{in} = 24.12 (.89) + .24 (.03) T_{out}$	82.9
e_{in} vs. e_{out}:		
All	$e_{in} = 2.55 (.11) + .79 (.14) e_{out}$	48.7
Winter only	$e_{in} = 2.28 (.12) + .87 (.31) e_{out}$	37.5
Summer only	$e_{in} = 3.03 (.16) + .45 (.16) e_{out}$	33.3

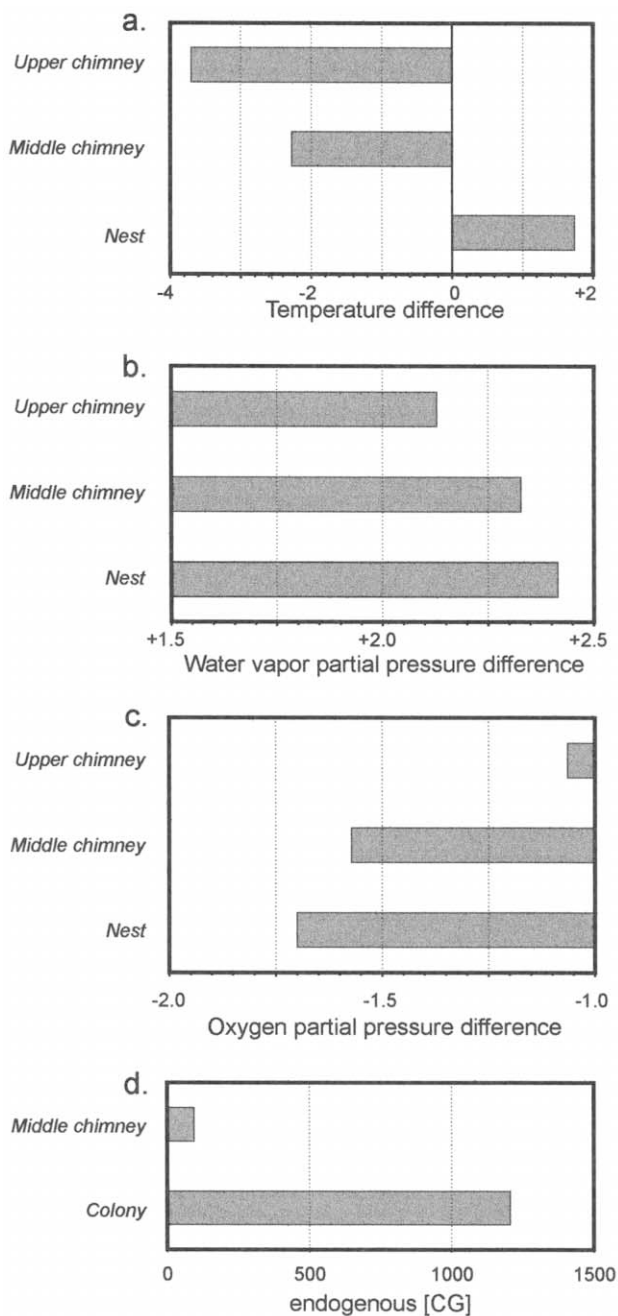Note. These data are for measurements taken from the nest only.

Figure 5. Regional variations in atmospheric composition in mounds of *Macrotermes michaelseni*. *a*, Temperature difference with ambient air ($T_{in} - T_{out}$ [°C]). *b*, Water vapor partial pressure difference with ambient air ($e_{in} - e_{out}$ [kPa]). *c*, Po_2 difference with ambient air ($Po_{2, in} - Po_{2, out}$ [kPa]). *d*, Endogenous combustible gas concentration in parts per million methane equivalents.

Table 3: Time constants for clearance of tracer gases from nests and mounds of *Macrotermes michaelseni*

	τ (min)	n
Season:		
Winter	5.69 (3.29)	14
Summer	8.09 (4.60)	17
Mound location:		
Nest	8.09 (4.60)	17
Middle chimney	13.29 (7.74)	11
Upper chimney	8.96 (4.07)	11

Note. Data are reported as mean (SD); $n =$ sample size.

seal (Fig. 4*d*). The shaft plug was a length of 40-mm PVC pipe, sealed on one end by a tight-fitting plastic cap (Fig. 4*c*). When the shaft plug was inserted into the shaft liner, the O-ring provided an air-tight seal between the liner's inside surface and the shaft plug's outside surface. To fit the shaft liner into a nest, a 2 1/2-inch-diameter hole was drilled into the mound or nest with a soil auger. The assembled shaft liner/shaft plug assembly was inserted into the hole and left in place for at least 12 h. During this time, the termites built around the outer face of the shaft liner, providing a tight seal around the shaft liner's outside surface. The internal sensor carriage was placed by sliding the shaft plug out and replacing it with the sensor carriage mounted on the end of a long piece of 40-mm-outer-diameter PVC pipe. In place, the sensor carriage was sealed from the outside air by both the O-ring seal and the soil seal built by the termites.

Interface. The interface served to deliver regulated power to the sensors, to sense and condition signals from the sensors, and to switch outputs from the sensors to the analog/digital converter. Switching was done through a digital multiplexer controlled either by a three-bit output (MGAS version 1) or a four-bit output (MGAS version 3) from the computer. Conditioning of the signals included zeroing and ranging of the outputs from the combustible gas sensors, conversion of the voltage from the oxygen sensor to partial pressure of oxygen, and temperature compensation of the relative humidity sensors.

Analog/Digital Conversion. Outputs from the interface were converted to digital form by an A/D converter (Remote Measurement Systems, Seattle) and transmitted to the computer through an RS 232 serial interface.

Computing and Data Logging. Control of the experiment and recording of the data was handled by a microcomputer (TRS 102, Tandy Corp, Houston). The computer controlled switching between sensors via a digital signal output to the A/D converter and interface. The computer also logged data as in-
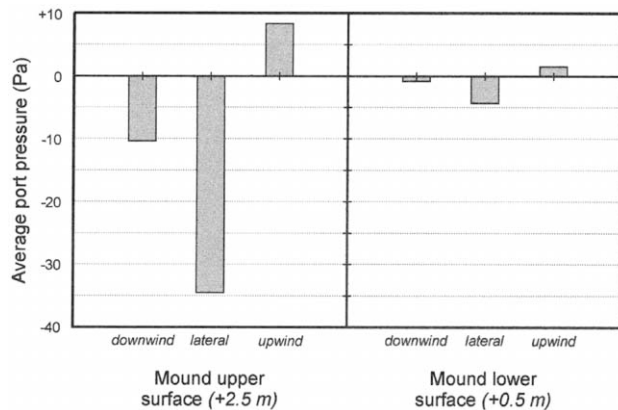
Figure 6. Wind-induced surface pressure over mounds of *Macrotermes michaelseni*. Pressures are reported as differences of pressure relative to still air. Left panel reports upwind, downwind, and lateral surface pressures at heights roughly 2.5 m above ground level. Right panel reports upwind, downwind, and lateral surface pressures at heights roughly 0.5 m above ground level.

dicated. The computer conducted experiments according to a set protocol. The typical protocol was as follows: (1) Before placing the sensors, data were logged every 30 s for 10 min with all sensors exposed to fresh air. These data provided a preexperiment baseline. (2) Following the placement of sensors into or onto the mound, data were logged every 30 s for 10 min. These data provided a preinjection baseline. (3) The tracer bolus was injected. (4) Data from the combustible gas sensors were recorded at time intervals of 30 or 60 s for a period of time, usually 1 h. In some experiments, postinjection data were logged for as long as 3 h. These data were the experimental results. (5) All sensors were removed from the mound and placed in fresh air, and their data were logged at 30-s intervals for an additional 10 min. These data provided correction for any drift in the sensors that arose from gradual loss of battery power. Drift was typically less than 5%.

Measurements of Wind Speed and Wind Direction. Wind speed was measured in two ways, depending upon available equipment. In the 1995 experiments, wind speeds were measured with a Dwyer handheld anemometer held into the wind. Wind

Table 4: Boundary layer wind speeds measured during summer and winter of 1998 (Namatubis study site)

Height above Ground (m)	Wind Speed (m s^{-1})
.5	.72 (.43)
1.5	1.38 (.64)
2.5	1.90 (.62)

Note. Data are reported as mean (SD).

direction was measured by taking the compass heading of a ribbon streamer tied to a pole or a branch of a nearby tree. In the 1996 experiments, wind speeds and wind directions at 2.5 m above ground level were measured using a cup anemometer and wind vane (Davis Instruments, Hayward, Calif.). In the 1997 experiments, wind speeds were measured at heights of 0.5, 1.5, and 2.5 m using three cup anemometers and wind vanes. In most experiments, wind speeds and directions were sampled synchronously with the sampling of combustible gas concentrations.

Measurements of Pressures on the Mound Surface and within the Mound. Pressures on the mound surface and within the surface conduits were measured using a multiplying micromanometer after the design of Vogel (1981). The manometer fluid was a soap solution mixed with a few drops of blue food coloring. During measurements, the manometer rested on a braced and leveled camp table set up next to the mound. The manometer itself was also equipped with leveling screws. Pressure ports were connected to a switching manifold that could direct as many as four different pressure differences to the micromanometer. In a typical configuration, the four pressure differences were port 1/port 2, port 1/ambient pressure, port 2/ambient pressure, and ambient pressure/ambient pressure. The last was used to zero the manometer. All pressures were differential pressure, not gauge pressure.
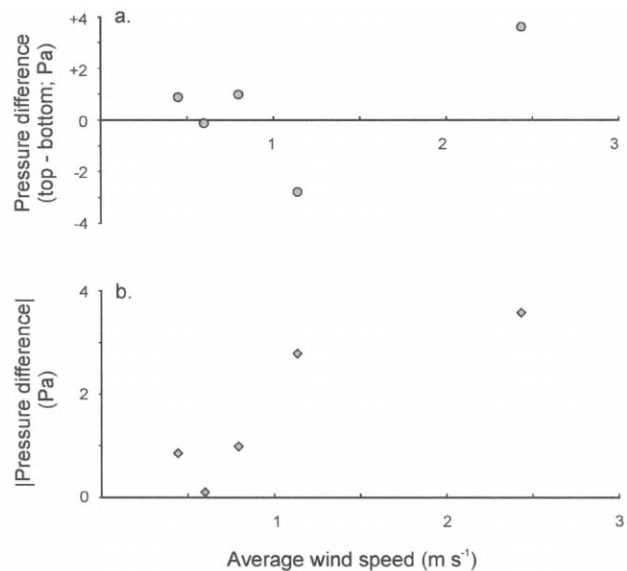

Figure 7. Vertical pressure differences in surface conduits as affected by variations of wind speed. *a*, Pressure difference between a pressure port at roughly 2.5 m above ground and a port at roughly 0.5 m above ground. A positive pressure difference indicates a downward-pointing pressure difference. *b*, Absolute pressure differences taken from *a*.
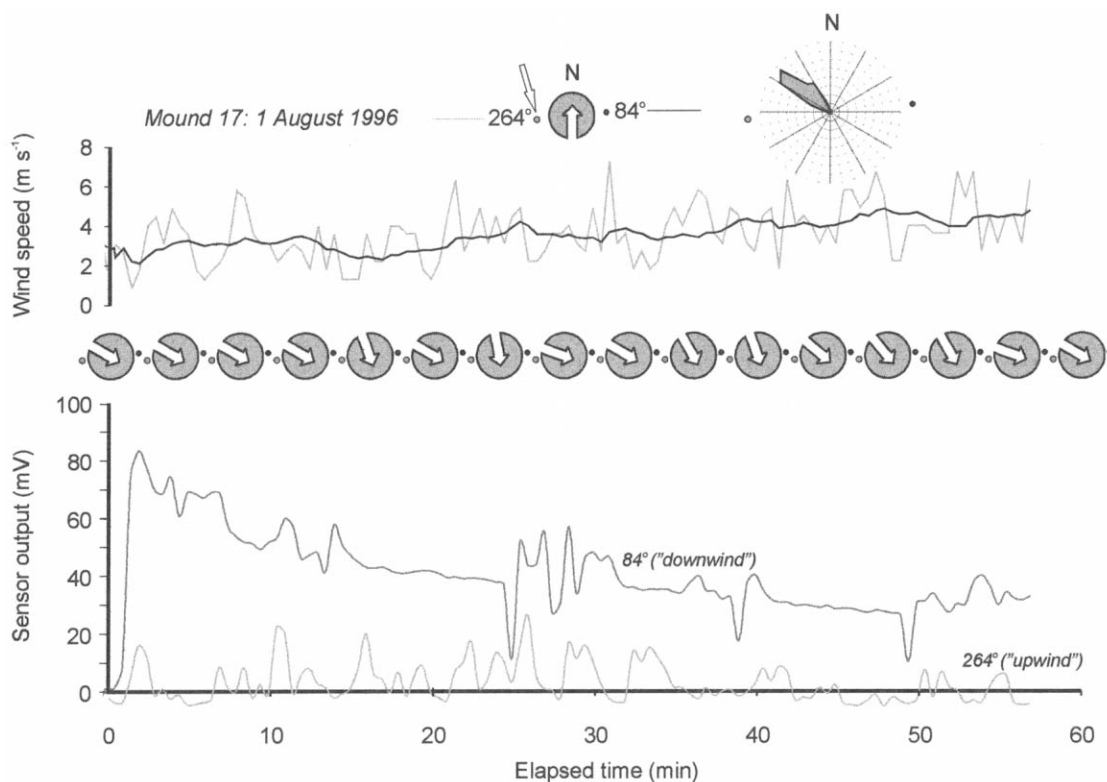
Figure 8. Pulse-chase experiment for mound 17 on August 1, 1996. Wind speeds averaged 3.5 m s^{-1}, intermittently freshening with gusts up to 7.2 m s^{-1}. Wind headings were steady out of the west-northwest (*wind rosette*) with a SD of 16° around the modal heading of 310°. Surface sensors were placed at compass headings of 84° ("downwind"; *black circles*) and 264° ("upwind"; *gray circles*). Injection point was into an upwind surface conduit, indicated by the unfilled arrow. Top panel is wind speed in meters per second. Gray line represents wind speeds at 30-s intervals. Black line represents the 5-min moving average of wind speed. Middle panel depicts compass cards indicating wind speed at 5-min intervals. Black and gray circles represent orientation of combustible gas sensors on the mound surface. Bottom panel graphs sensor output of the designated sensors in millivolts.

Wind-induced surface pressures were measured at ports placed about a centimeter off the mound surface at any of six locations: upwind (within ±60° of the wind heading), lateral to the wind (between ±60° and ±120° of the wind heading), and downwind ($>±120°$ of the wind heading) at roughly 2.5 and 0.5 m above ground level. Pressure ports were constructed from a center-drilled plastic rod tapped into a 1/4-inch plastic hose barb. A thick-walled plastic tube connected the pressure

Table 5: Densities of air at various localities within the mounds of *Macrotermes michaelseni*

	Nest	Middle Chimney	Upper Chimney
P$_{O_2}$ (kPa)	16.36 (.75)	16.34 (.60)	16.87 (.34)
P$_{CO_2}$ (kPa)[a]	1.58 (.70)	1.60 (.61)	1.09 (.31)
P$_{H_2O}$ (kPa)	3.40 (.43)	3.13 (.38)	2.86 (.63)
P$_{N_2}$ (kPa)[a]	64.99 (.38)	65.26 (.38)	65.51 (.60)
MW (g mol^{-1})[a]	28.67 (.075)	28.70 (.078)	28.66 (.064)
T_{in} (°C)	31.97 (2.82)	32.95 (2.11)	33.24 (2.22)
Molar V (m^3 mol^{-1})[a]	.02939 (.0002)	.02948 (.0002)	.02951 (.0002)
ρ (kg m^{-3})[a]	.976 (.009)	.974 (.008)	.971 (.008)

Note. Data are reported as mean (SD). Nominal atmospheric pressure at Namatubis is 86.33 kPa.
[a] Estimates.

port to the switching manifold that in turn connected to the ports of the micromanometer.

Internal pressures were measured using the pressure ports described above but with a shaft liner/shaft plug arrangement similar to that for the internal sensors. About 12 h before an experiment, a 1-inch-diameter shaft was sunk into the mound until it reached a tunnel, and a shaft liner/shaft plug assembly was placed. Injury to the mound was healed by the termites as described above. To measure pressure, the plug was removed and replaced with a pressure port. One shaft liner was placed high up on the mound about a meter above another port placed low on the mound.

Pressures were measured using a protocol that recorded wind speed, wind direction, and pressure every 30 s for a period of 10 min. Each round of measurement included one with the switching manifold in the atmosphere-atmosphere configuration to correct for drift in the manometer.

Estimating Air Densities

Air densities and buoyant forces within the nest and mound were estimated from measurements of local P_{O_2}, P_{H_2O} (both in kPa), and air temperature (°C). Estimates of air density involved first inferring the molar composition of the local atmosphere and, from this, estimating the air's average molecular weight (MW_{air}). Density is calculated from MW_{air} and molar volume.

The atmospheric pressure (P_a), which at Namatubis is nominally 86.33 kPa, comprises the partial pressures of the gases in the atmosphere:

$$P_a = P_{N_2} + P_{O_2} + P_{CO_2} + P_{H_2O}. \tag{1}$$

Both P_{O_2} and P_{H_2O} were measured. The P_{CO_2} is estimated from the depletion of oxygen in the nest atmosphere, $\Delta P_{O_2} =$
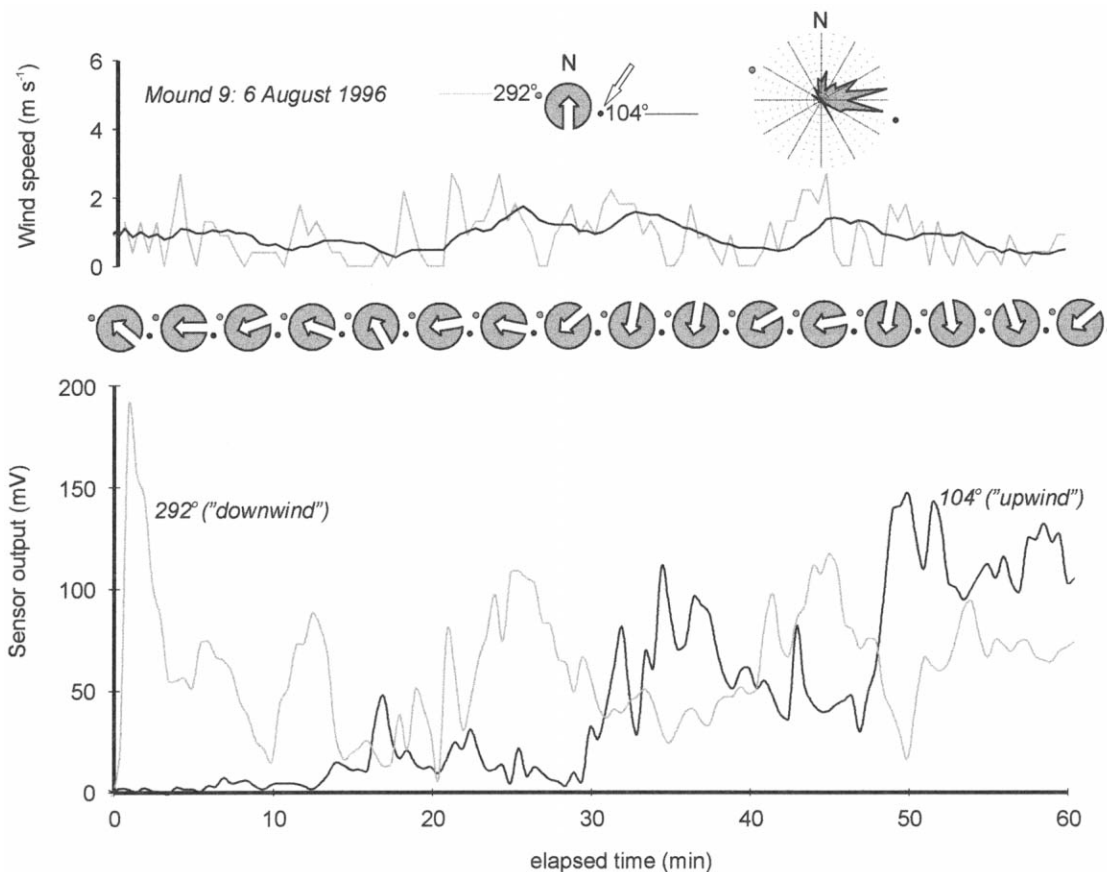

Figure 9. Pulse-chase experiment for mound 9 on August 6, 1996. Wind speeds average 0.9 m s^{-1}, freshening with occasional gusts up to 2.7 m s^{-1}. Wind headings were predominantly out of the east and highly variable, most commonly easterly, with a SD of wind direction of 58° with respect to modal wind direction of 80°. Surface sensors were placed at compass headings of 292° ("downwind"; *gray circles*) and 104° ("upwind"; *black circles*). Injection point was into an upwind surface conduit, indicated by the unfilled arrow. Conventions as in Figure 8.

Table 6: Maximum average and maximum summed combustible gas concentrations at surface conduits of mounds of *Macrotermes michaelseni*

Position on Mound Surface	Low	High
Maximum average CG	1.9 (2.4)	4.6 (6.4)
Wind heading relative to maximum average CG[a]	109 (47)	124 (38)
Maximum summed CG	13.2 (23.1)	31.2 (39.0)
Wind heading relative to maximum summed CG[a]	108 (44)	105 (49)

Note. Tabulated data grand averages of the maximum average CG and maximum summed CG for all mounds measured and SDs of the averages. CG is in parts per million. Sensors at a "high" location are positioned at least 2 m above ground level. Sensors at a "low" location are positioned no higher than 1 m above ground level.

[a] In absolute degrees relative to sensor.

$P_{O_2, atm} - P_{O_2, nest}$. Assuming a respiratory quotient of 0.8 (Peakin and Josens 1978), the elevation of P_{CO_2} or $\Delta P_{CO_2} = -0.8 \Delta P_{O_2}$. The P_{CO_2} in the nest is therefore

$$P_{CO_2, nest} = P_{CO_2, nest} - 0.8 \Delta P_{O_2}. \tag{2}$$

The atmospheric P_{CO_2} at Namatubis was presumed to be 0.03 kPa. The P_{N_2} is then estimated as

$$P_{N_2} = P_a - P_{O_2} - P_{CO_2} - P_{H_2O}. \tag{3}$$

From these pressures, the mole fractions (mf) of each gas are estimated:

$$mfN_2 = P_{N_2}/P_a, \tag{4a}$$

$$mfO_2 = P_{O_2}/P_a, \tag{4b}$$

$$mfCO_2 = P_{CO_2}/P_a, \tag{4c}$$

$$mfH_2O = P_{H_2O}/P_a. \tag{4d}$$

The average molecular weight of the air (MW_{air}; kg mol^{-1}) is estimated from the mole fractions and molecular weights of the respective gases:

$$MW_{air} = mfN_2 \, MWN_2 + mfO_2 \, MWO_2$$
$$+ mfCO_2 \, MWCO_2 + mfH_2O \, MWH_2O. \tag{5}$$

The molar volume of the gas, V_M (m^3), is estimated from the ideal gas law:
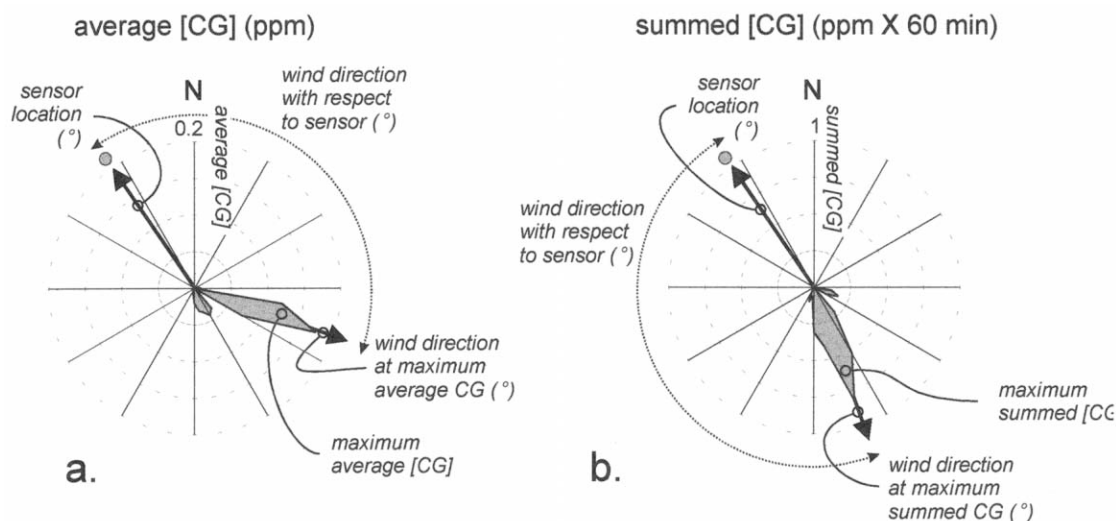
$$V_M = \frac{RT}{P_a}, \tag{6}$$

Figure 10. Schematic diagram for calculation of maximum average CG (*a*) and maximum summed CG (*b*) and wind directions relative to sensor position. Wind rosettes indicated average CG or summed CG with respect to wind direction. Radial axis represents the average CG or summed CG for a particular sensor (*gray circle*) over a period of 60 min postinjection. Directional axis represents compass headings of wind direction. Average CG or summed CG is calculated for each 15° interval of wind direction and plotted on the wind rosette (*gray-filled polygon*). Maximum average CG and maximum summed CG are identified as indicated in this figure. Wind direction relative to sensor position is the shortest arc between the wind heading at which maximum average or maximum summed CG occurs and the compass heading of the sensor.
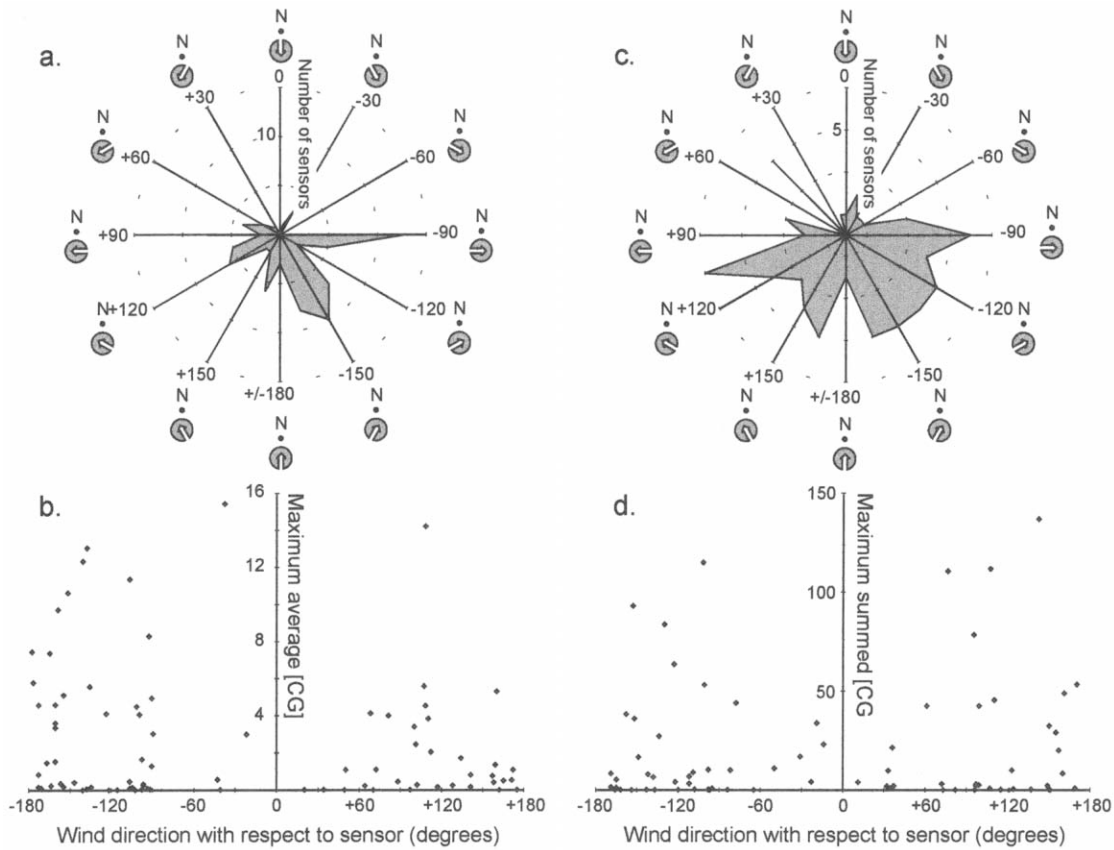
Figure 11. Distributions of maximum average CG (*a*, *b*) and maximum summed CG (*c*, *d*) for 10 mounds measured in austral summer 1997. Top panels (*a*, *c*) plot numbers of sensors in each interval of relative wind direction at which maximum average or maximum summed CG occurs. Bottom panels (*b*, *d*) plot the values of maximum average CG and maximum summed CG against relative wind direction for each sensor.

where T is temperature in Kelvins, and R is the gas constant (8.314 J mol^{-1} K^{-1}). Density (ρ; kg m^{-3}) is simply the ratio of the air molecular weight and the molar volume:

$$\rho = \frac{MW_{air}}{V_M}. \tag{7}$$

The tendency of a density difference to drive a flow is given by the dimensionless Grashof number, Gr (Vogel 1981). For a density difference between air in the nest and chimney, for example, the Grashof number is

$$Gr = \frac{\rho_{ch}^2 g (\rho_{ch} - \rho_{nest})}{\rho_{nest} \mu^2}, \tag{8}$$

where ρ_{nest} = density of air in the nest (kg m^{-3}), ρ_{ch} = density of air in the chimney, g = gravitational acceleration (9.8 m s^{-2}), and μ = the air dynamic viscosity (1.85e − 5 kg m^{-1} s^{-1}). The density difference is presumed to be distributed

over a distance of 1 m. Grashof numbers are commonly quite large, with transitions between laminar and turbulent flows occurring at values of 10^5 to 10^6.

Results

Composition of the Nest Atmosphere

The nest atmosphere differed in composition and temperature from the outside air and varied significantly with season (Table 1). In summer, nest air was about 6°C warmer than in winter ($F_{1,47} = 6.18$, $P = 0.017$). Nest air temperature was also damped compared to external temperature, as indicated by the slope of the regression of nest air temperature versus outside air temperature (Table 2). Nest air temperature was significantly more damped in summer than in winter ($t_{47} = 3.67$, $P < 0.001$), with a summer slope roughly 69% that in winter (Table 2).

Absolute humidity of the nest atmosphere was always higher than outside (Table 1). For both nest and outside air, absolute humidities were higher in summer than in winter (Table 1).
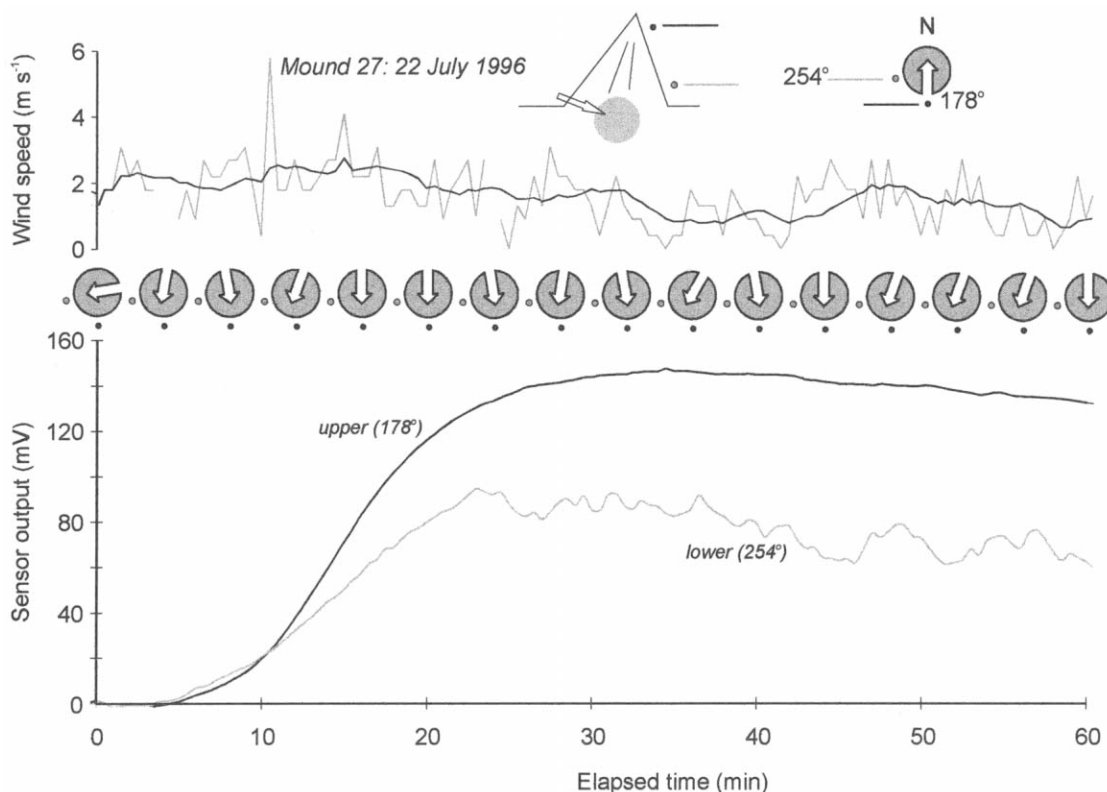
Figure 12. Pulse-chase experiment for mound 27 on July 22, 1996. Winds were mild, averaging 1.64 m s^{-1} with a SD of 0.9 m s^{-1}. There were occasional gusts as high as 5.8 m s^{-1}, and winds dropped to null. Wind directions were also steady out of the north with a modal bearing of 0° and a SD with respect to the modal wind direction of 19°. Two surface sensors were placed: one high (*black circle*) and one low (*gray circle*). The high sensor was placed downwind at a compass direction of 178°, while the low sensor was placed downwind-lateral to wind at a compass direction of 254° (*solid gray*). Other conventions as in Figure 8.

However, relative humidity of nest air was about 70% in both winter and summer, indicating that the higher summer absolute humidity was due primarily to warmer temperatures. Nest humidity was less strongly damped than temperature; for both summer and winter data combined, the average slope of e_{in} versus e_{out} was 0.79, compared to a slope of T_{in} versus T_{out} of 0.36 (Table 2). In summer, the slope of e_{in} versus e_{out} was roughly half that in winter (Table 2), indicating that internal humidity was more strongly damped in summer than in winter ($t_{31} = 3.00$, $P = 0.003$).

Po$_2$ in the nest air averaged about 1.7 kPa below atmospheric Po$_2$ and did not differ between winter and summer ($F_{1,48} = 2.34$, $P = 0.132$).

Endogenously produced combustible gas, probably methane, was present in the nest air, averaging about 1,200 ppm methane equivalents over the year (Table 1). Endogenous combustible gas concentrations did not differ significantly between summer and winter ($F_{1,20} = 0.138$, $P = 0.715$).

By any measure, mound size had no statistically discernible

effect on temperature, humidity, or oxygen concentration of the nest air.

Regional Variation in Composition of the Nest Atmosphere

Composition of the chimney air differed significantly from that of the nest air. Measurements of humidity, temperature, and Po$_2$ in the chimney are available for the summer months only. Endogenous combustible gas concentrations were measured in both summer and winter.

Chimney air temperature is statistically indistinguishable from nest air temperature ($F_{2,39} = 1.67$, $P = 0.201$; Fig. 5). Nest air is more humid than chimney air, but the difference is marginally significant ($F_{2,38} = 2.81$, $P = 0.072$; Fig. 5). When humidity variation due to variations in external humidity is accounted for, chimney humidity is significantly less than nest humidity ($F_{2,38} = 4.60$, $P = 0.016$). Oxygen concentrations were lowest in the nest and middle chimney but were about 500 Pa higher in the upper chimney (Fig. 5), the difference
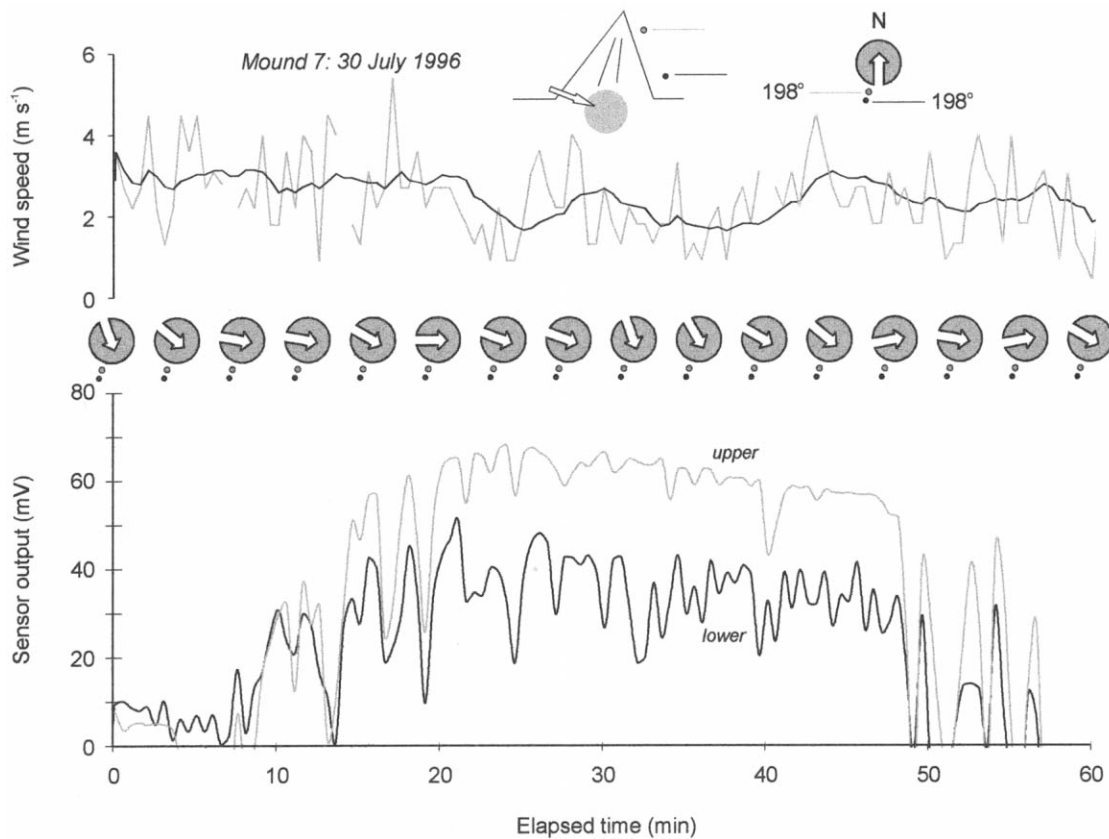
Figure 13. Pulse-chase experiment for mound 7 on July 30, 1996. Winds were brisk and variable, averaging 2.4 m s^{-1} with a SD of 1.02 m s^{-1}. Gusts were up to 5.4 m s^{-1}, but wind speeds never dropped below 0.4 m s^{-1}. Wind direction was variable out of the northwest with a modal heading of 300° and a SD of 25° with respect to modal. Two surface sensors were placed: one high (*gray circles*) and one low (*black circles*), both at a compass direction of 198°. Tracer was injected into the nest. Other conventions as in Figure 8.

being marginally significant ($F_{2,39} = 2.71$, $P = 0.079$). Finally, endogenous combustible gas differed significantly between nest and chimney ($F_{1,38} = 25.52$, $P < 0.001$), dropping from about 1,200 ppm methane equivalents in the nest to about 90 ppm methane equivalents in the chimney (Fig. 5).

Clearance Rates for Tracer Gases from the Nest and Mound

Tracer in the nest cleared with an average time constant of 7.00 min, ranging from 1.8 to 18.3 min, and did not differ significantly between winter and summer ($F_{1,29} = 2.68$, $P = 0.112$; Table 3). Tracer cleared at different rates from different localities in the mound ($F_{2,36} = 3.13$, $P = 0.056$; Table 3). In the nest and in the upper parts of the chimney, the clearance time constant averaged about 8.5 min (Table 3). The chimney just above the nest appeared to be relatively stagnant, with clearance time constants averaging slightly over 13 min (Table 3). Mound size had no statistically discernible influence on time constants for clearance from the nest.

Surface and Surface Conduit Pressures

Wind induces a complex distribution of pressure over the mound's surface (Fig. 6). Close to the ground, surface pressures were significantly stronger than higher on the mound ($F_{1,948} = 38.2$, $P < 0.001$), reflecting the boundary layer variation of wind speeds ($F_{2,111} = 32.8$, $P < 0.001$; Table 4). Surface pressure also varied significantly with position on the mound ($F_{2,948} = 71.0$, $P < 0.001$). At upwind mound surfaces, pressures were positive (Fig. 6), while at downwind and lateral surfaces, pressures were negative, the strongest suction pressures being at the mounds' flanking surfaces (Fig. 6).

Pressure differences were evident along the surface conduits and ranged from about +8 to −5 Pa from top to bottom of the mound (Fig. 7). Most commonly, surface conduit pressure was higher at the top of the mound than the bottom, but in two instances, the pressure difference was reversed. The pressure difference showed no significant relation with wind speed ($F_{1,3} = 1.17$, $P = 0.358$; Fig. 8*a*), but the absolute pressure dif-
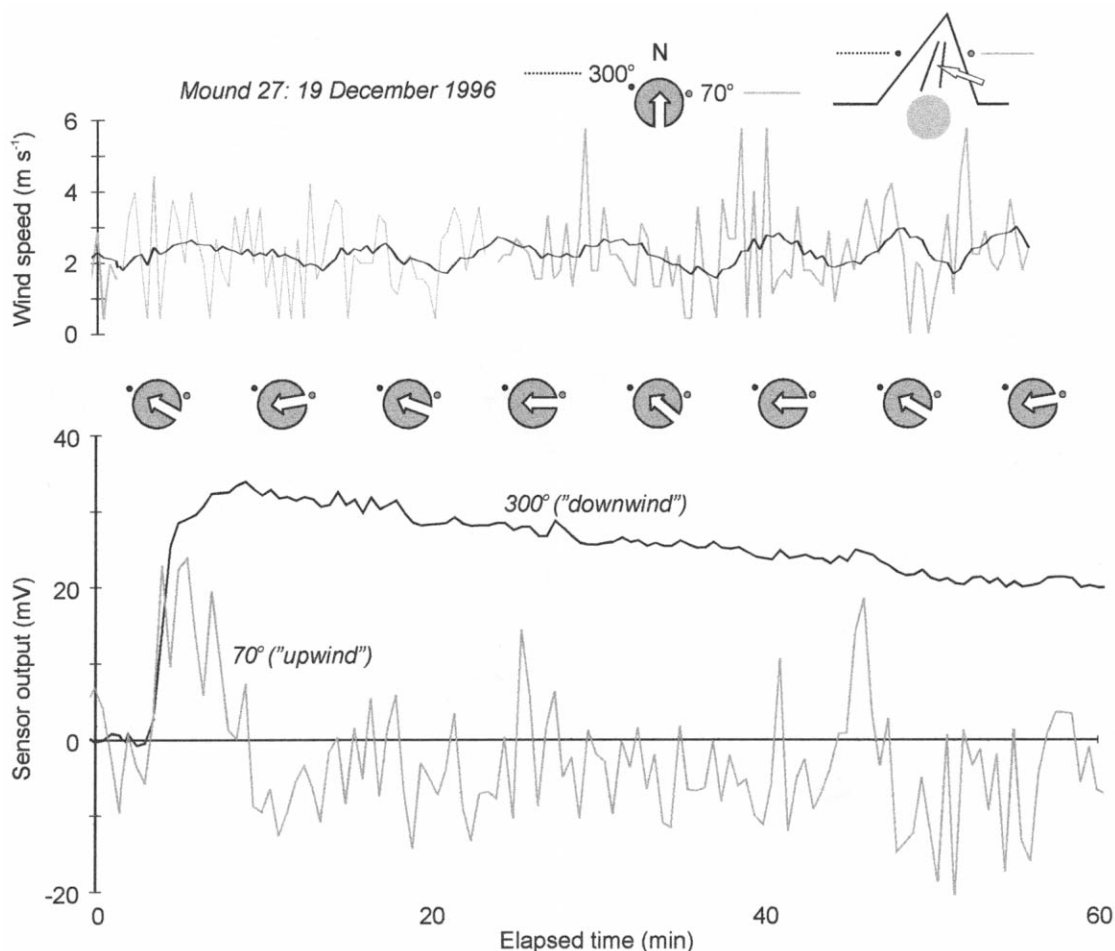
Figure 14. Pulse-chase experiment for mound 27 on December 19, 1996. Winds were brisk and variable, averaging 2.29 m s^{-1} with a SD of 1.17 m s^{-1}. Wind was variable out of the southeast with an average bearing of 106°, ranging from 80° to 130°. Two surface sensors were placed: one upwind at a compass direction of 70° (*gray circle*) and one downwind at a compass direction of 300° (*black circle*). Tracer was injected into the middle chimney. Other conventions as in Figure 8.

ference (i.e., the pressure difference without regard to its direction) was significantly correlated with wind speed ($F_{1,3} = 10.59$, $P = 0.047$; Fig. 8b).

Estimated Air Densities in the Chimney and Nest

Estimated air densities throughout the mound averaged about 0.974 kg m^{-3}, and there were no statistically discernible differences between the nest and chimney ($F_{2,37} = 0.794$, $P = 0.460$; Table 5).

Patterns of Air Movement in Nest and Mound

Air movements in the nest and mound were complex. In the following results, commonly observed patterns of flow are presented as a description of the pattern, followed by results that

support the assertion. Usually, these are representative results from a pulse-chase experiment on a particular mound.

The Surface Conduits Constitute at Least One Well-Mixed Air Space That Is Stirred by Wind. If a bolus of tracer was injected into a surface conduit, the tracer typically migrated rapidly to downwind surface conduits, irrespective of whether tracer was injected into an upwind or downwind conduit.

Consider the results from mound 17 (Fig. 8). Despite being injected close to the upwind sensor, tracer did not appear there in appreciable amounts but concentrated strongly at the downwind sensor within 2 min following the injection. Following its initial appearance in the downwind surface conduits, tracer then made intermittent appearances at the upwind sensor (at about 16–18, 26–28, 36–40, and 48–50 min), which were cor-
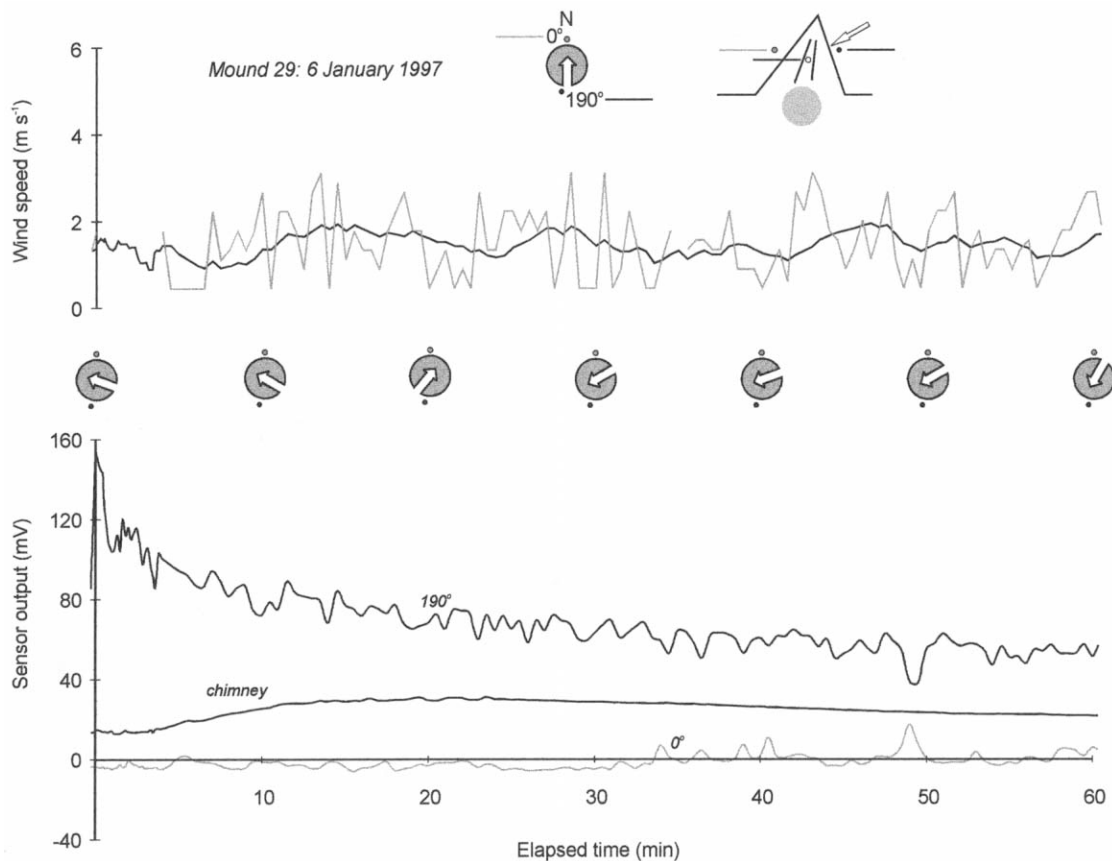
Figure 15. Pulse-chase experiment for mound 29 on January 6, 1997. Winds were light, averaging 1.5 m s^{-1} with a SD of 0.75 m s^{-1}. Wind was variable out of the east with a mean heading of 90°, ranging from 30° to 220°. Three sensors were placed: two at the surface at compass directions of 0° (*gray circles*) and 190° (*black circles*) and one in the chimney (*open circle*). Tracer was injected into a surface conduit near the sensor at 190°. Other conventions as in Figure 8.

related with shifts of wind direction that brought wind lateral to both sensors.

Compare the mound 17 results with those from mound 9 (Fig. 9). During this experiment, winds were milder, with more variable wind directions. A bolus of tracer was injected into a conduit below the initially upwind sensor (located at 104°), and tracer migrated quickly to the downwind surface conduit (located at 292°), as it did for mound 17 (Fig. 8). At about 32 min postinjection, the wind shifted, bringing wind lateral to both surface sensors. There was a clear and rapid migration of tracer from the sensor at 292° toward the sensor at 104°. Following other shifts in wind direction, back to easterly at about 40 min postinjection and again back to northerly at about 50 min postinjection, tracer migrated rapidly to whichever sensor was downwind or lateral to wind. Thus, variations of wind direction induce a "sloshing" movement of air back and forth in the conduits.

Exchange of Gas between the Nest and Mound Surface Is Strongly

Influenced by Wind Direction and by Boundary Layer Variation of Wind Speed. The mound experiences strong suction pressures at the downwind and lateral-to-wind surfaces and significant positive pressures at the upwind surface (Fig. 6). These pressures affect how gases are distributed in the surface conduits (Figs. 8, 9).

Ten mounds were outfitted with from six to 10 surface combustible gas sensors, positioned at several compass orientations on the mound, and at two vertical positions: "high" and "low" (2.5 and 0.5 m above ground level, respectively). A bolus of tracer was injected into the nest or mound, and its appearance at the surface sensors correlated with wind direction for 60 min following injection. Tracer emissions were correlated with wind direction as follows (Fig. 10). Each sensor's position on the mound was designated by its compass heading. Following the injection of tracer, combustible gas concentration at each sensor was measured every 30 s for 1 h. Wind directions were recorded synchronously. Data for each sensor were summed, averaged,
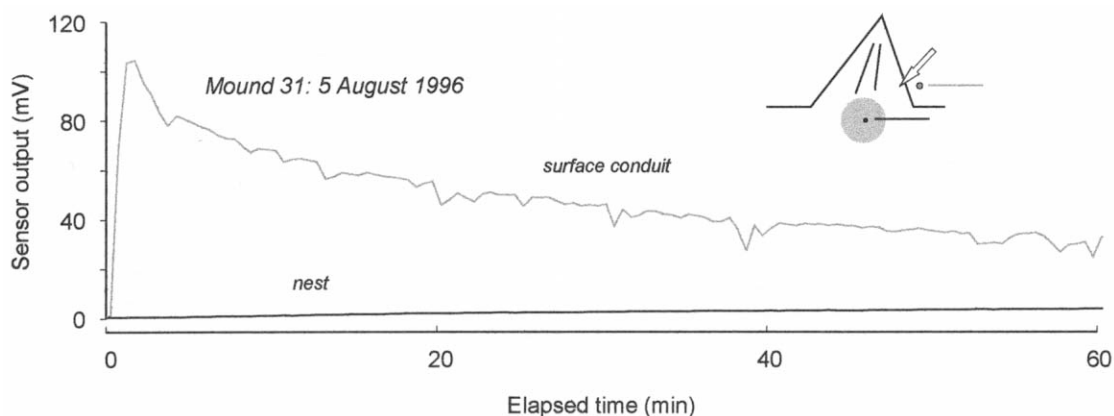
Figure 16. Pulse-chase experiment for mound 31 on August 5, 1996. Winds were mild and steady, averaging 1.5 m s^{-1} with a SD of 0.65 m s^{-1}. Winds were variable out of the southeast with a modal heading of 130° and a SD with respect to the mode of 28°. One surface sensor was placed (*gray circle*) at which tracer was injected. A sensor was also placed into the nest (*black circle*). Other conventions as in Figure 8.

and plotted against wind direction (Fig. 10). The wind heading at which average or summed combustible gas concentration (CG) was maximum was then identified. The wind direction of these maxima with respect to the sensor's position was then calculated as the shortest arc between these wind compass headings and the sensor's compass position (Fig. 10).

Tracer migrates from the nest preferentially to the lateral and downwind surfaces of the mound (Fig. 11; Table 6). Tracer emerged most strongly at sensors that were oriented from 105° to 124° with respect to wind, irrespective of height (maximum average CG: $F_{1,69} = 2.32$, $P = 0.13$; maximum summed CG: $F_{1,60} = 0.10$, $P = 0.74$). Tracer also emerged strongly from surfaces high off the ground (maximum average CG: $F_{1,69} = 4.58$, $P = 0.036$; maximum summed CG: $F_{1,60} = 4.53$, $P = 0.037$). It is rare to see a maximum average CG or maximum summed CG appearing at a wind heading more acute than 90° relative to the sensor (Fig. 11). The one instance in which this did occur followed very heavy rains that left the mound surface soaked and, presumably, its surface permeabilities compromised. A similar conclusion follows from plots of the maximum average and maximum summed CGs with respect to wind heading (Fig. 11). The highest values accumulate at wind headings greater than ±90° relative to the sensor.

Gas Moves Slowly from the Nest to the Surface Conduits. Movement of tracer from the nest to the surface conduits is slow compared to its rapid distribution within the surface conduits. The result seen for mound 27 is typical (Fig. 12). Both sensors were located downwind and lateral to the wind direction. Following injection into the nest, tracer first appears at the surface conduits in about 5 min and peaks at about 35–40 min postinjection. In this instance, tracer migrated preferentially to the upper surface conduit. A similar pattern is seen in the exper-

iment on mound 7 (Fig. 13). Again, tracer slowly made its way from the nest to the surface, first appearing at about 8 min postinjection and reaching a peak concentration at 28–30 min. Mound 7 experienced more vigorous and gustier winds than mound 27, which makes mound 7's clearance curves (Fig. 13) "choppier" than mound 27's (Fig. 12).

There is a Two-Way Exchange between the Surface Conduits and Chimney That Is Strongly Damped. Air moves between the surface conduits and chimney through the network of lateral connectives. Consider first the experiment with mound 27 (Fig. 14). One surface sensor (at 300°) was downwind through the entire experiment, and the other (at 70°) was consistently upwind. Following injection into the middle chimney, tracer appeared rapidly first at both upwind and downwind sensors, after which tracer was redistributed largely to the downwind sensor, reaching peak concentration at about 7 min. Although tracer stayed predominantly near the downwind sensor, when winds freshened at about 30 and 40 min postinjection, slight "puffs" of tracer appeared at the upwind sensor. In the experiment on mound 29 (Fig. 15), tracer injected into a surface conduit migrated to the chimney but only slowly, reaching peak concentration there after roughly 20 min.

Thus, there appears to be a hysteresis that favors movements of air from the chimney to the surface conduits but disfavors movements the other way. It is also interesting that the flows of air between chimney and surface conduit are damped considerably compared to movements of gas within the surface conduits themselves. Compare the highly variable concentrations observed for gas movements in the surface conduits (Figs. 13–15) with the relatively smooth clearance curves in Figures 14 and 15. This suggests the reticulated network of lateral con-
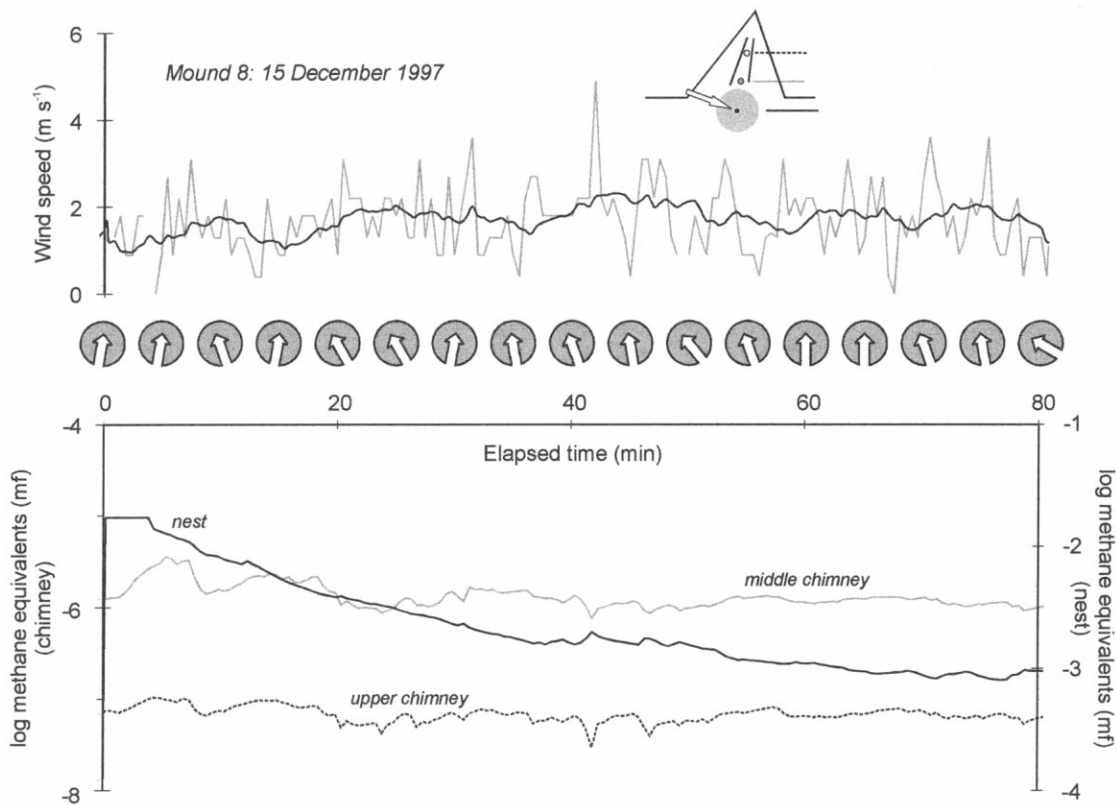
Figure 17. Pulse-chase experiment for mound 8 on December 15, 1997. Winds were brisk, averaging about 1.75 m s^{-1} with gusts up to 4.8 m s^{-1}. Wind direction was steady out of the south-southeast. Internal sensors were placed in the nest (*black circle*), middle chimney (*gray circle*), and upper chimney (*open circle*). Tracer was injected into the nest. Other conventions as in Figure 8.

nective tunnels serve to damp the movements of air between the chimney and surface conduits.

There Is Little Movement of Tracer Gas from the Surface Conduits Back to the Nest. Circulation of air in the mound should return tracer injected into a surface conduit back to the nest. No such flow was observed. In the experiment with mound 31 (Fig. 16), a bolus of tracer injected into a downwind surface conduit registered there strongly but did not appear in the nest.

Air Moves Both Ways between the Chimney and Nest and Is Influenced by Variations of Wind Speed. Tracer moves both from the nest to the chimney and vice versa, but there appears to be a hysteresis in the rates of movement. Tracer moves quickly into the lower chimney from the nest, as indicated in the experiment on mound 8 (Fig. 17). Following injection of tracer into the nest, it appears in the middle chimney in about 5 min and oscillates in rough synchrony with wind, rising in concentration during lulls and falling when the wind freshens (Fig. 17). There is little evidence of a pulse in the upper chimney. When tracer is injected into the middle chimney, as it is for

mound 2 (Fig. 18), there is a slight migration of tracer back to the nest, reaching a peak concentration there at 20–40 min postinjection. A particularly interesting feature of this experiment is the effect of wind on clearance of tracer from the chimney. On Figure 18, I have plotted a series of horizontal bars, indicating times when wind speed was higher than average (high bars) and lower than average (low bars). During periods of above-average winds, clearance of tracer from the chimney noticeably accelerated. Note also at the lull in the wind from roughly 35 to 45 min postinjection, tracer concentration rose in the chimney, fed perhaps by back flow of gas from the surface conduits. This pulse could not have arisen from the nest because tracer concentrations were always lower in the nest.

The Overall Pattern of Air Movements in the Mound Is Highly Complex and Strongly Driven by Wind. Some of the complexity of air movements in the mound and nest can be appreciated by experiments that could monitor CG at many locations in and around the mound and nest. These records are very detailed, and only two are presented here as examples. In the experiment with mound 23 (Fig. 19), tracer was injected into
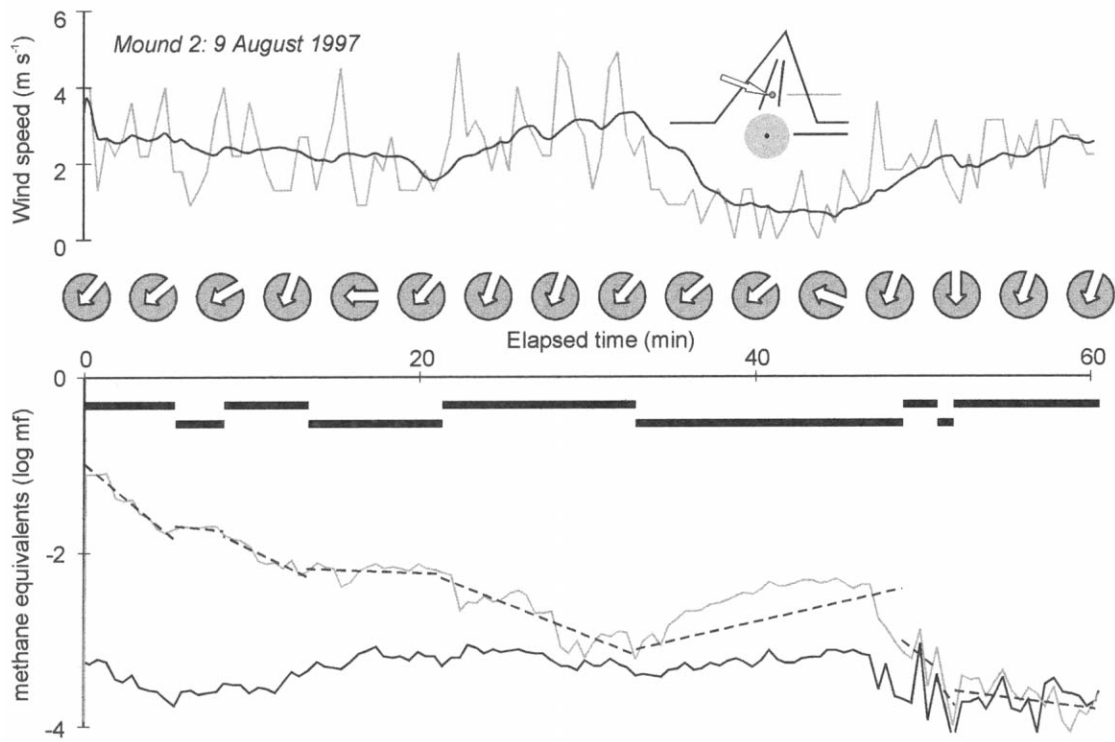
Figure 18. Pulse-chase experiment for mound 2 on August 8, 1997. In this experiment, winds were brisk and variable, averaging 2.1 m s^{-1} with a SD of 1.03 m s^{-1} and gusts up to 4.8 m s^{-1}. Wind directions were variable out of the northeast. Internal sensors were placed in the middle chimney (*gray circle*) and the nest (*black circle*). Tracer was injected into the middle chimney. Heavy solid lines along the top indicate periods when winds were higher than the average (*upper*) or lower than the average (*lower*). Dashed lines laid over the trace for chimney combustible gas concentration indicate the clearance rates during periods of higher-than-average or lower-than-average winds. Other conventions as in Figure 8.

the nest, and its movements monitored with sensors in the chimney and at several surface locations. The second experiment, with mound 44 (Fig. 20), was similar except tracer was injected into the chimney rather than the nest.

Tracer injected into the nest appeared rapidly in the chimney and then was distributed mostly to the upper surface conduits, reaching peak concentrations at about 18–25 min postinjection (Fig. 19). Tracer appeared to be distributed uniformly from the chimney to the upper surface conduits, seemingly without respect to wind direction; there was a strong pulse at the sensor at 109°, which was upwind through most of the experiment, and also at the sensors at 0° and 339°, both of which were commonly downwind. Also noteworthy is the absence of tracer in some of the upper surface conduits, such as the sensor at 256°. Only after about 40 min postinjection does tracer begin to appear at the lower surface conduits and, with one exception (the sensor at 109°), at low concentrations. Finally, the strong oscillations in tracer concentration in the chimney are strongly correlated with oscillations of wind speed, with lulls in the wind corresponding to increases of tracer in the chimney and with

freshening of the wind corresponding to a decline of tracer in the chimney.

Tracer injected into the chimney (Fig. 20) shows a slow and slight migration of tracer back into the nest. Again, tracer injected into the chimney migrates preferentially to the upper surface conduits, although a strong initial pulse is seen in one of the lower surface conduits (the sensor at 197°). Wind directions during this experiment were highly variable, and the "sloshing" action is clearly evident at the sensors at 32°, 221°, and 248°.

Discussion

Three conclusions follow from the results reported here. First, thermosiphon ventilation does not operate in the mounds and nests of *Macrotermes michaelseni*. Rather, the colony's gas exchange is driven by a complex interaction between architecture of the mound and nest, kinetic energy in wind, and metabolism-induced natural convection within the nest. Second, ventilatory movements of air in the mound and nest are
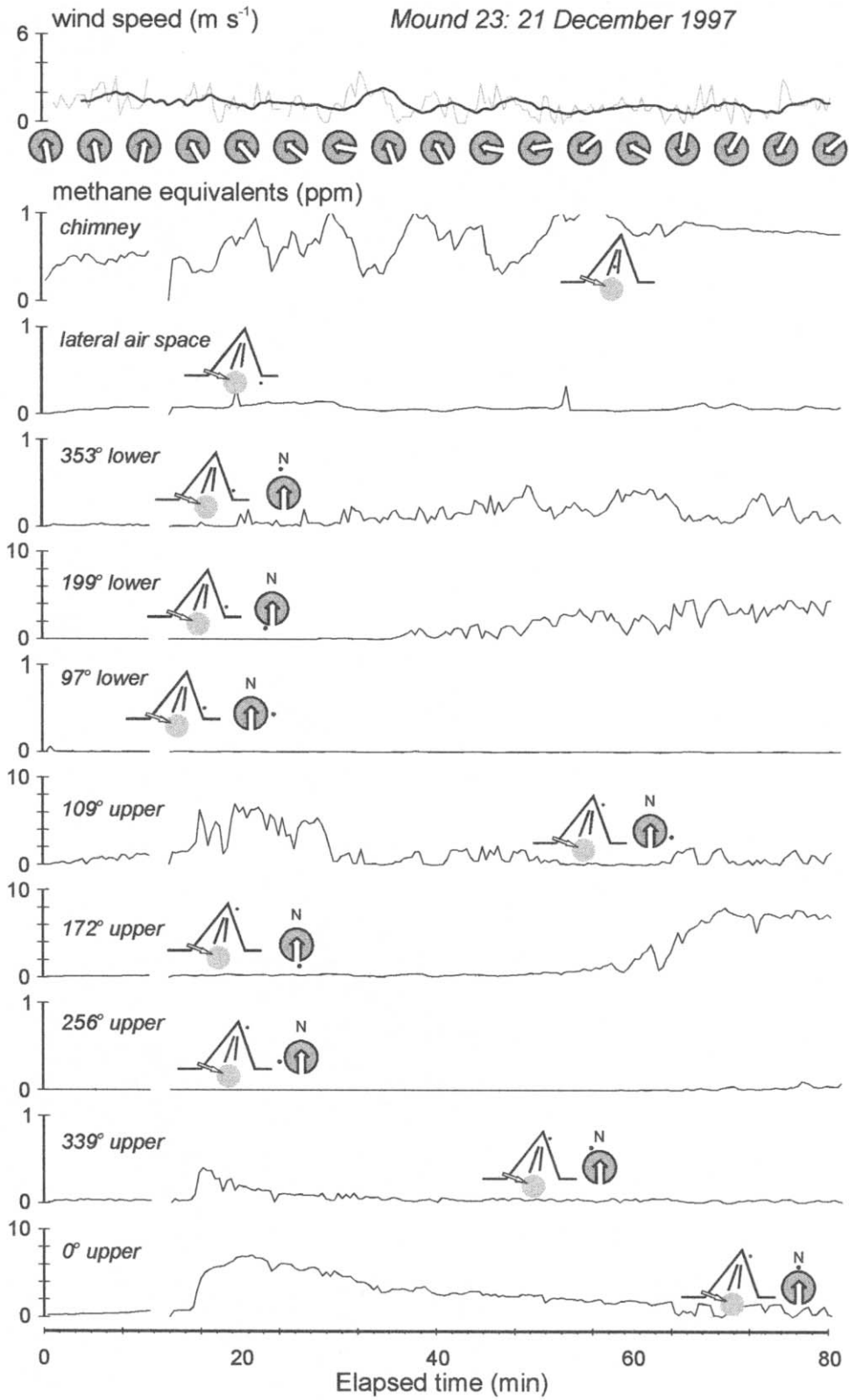
Figure 19. Pulse-chase experiment for mound 23 on December 21, 1997. Sensors were placed at several localities indicated by the filled circles on the cartoons accompanying each trace. Tracer was injected into the nest. Other conventions as in Figure 8.
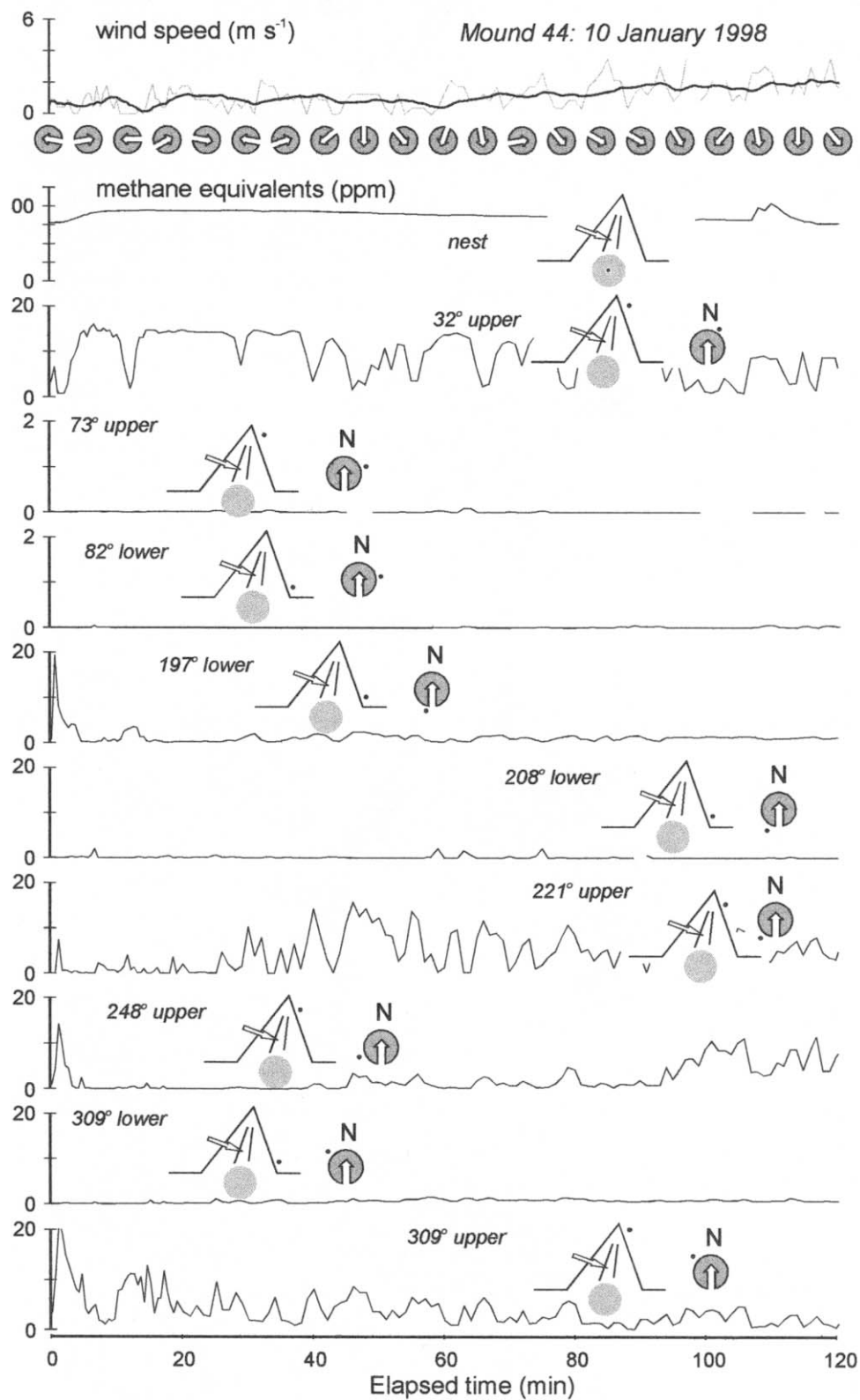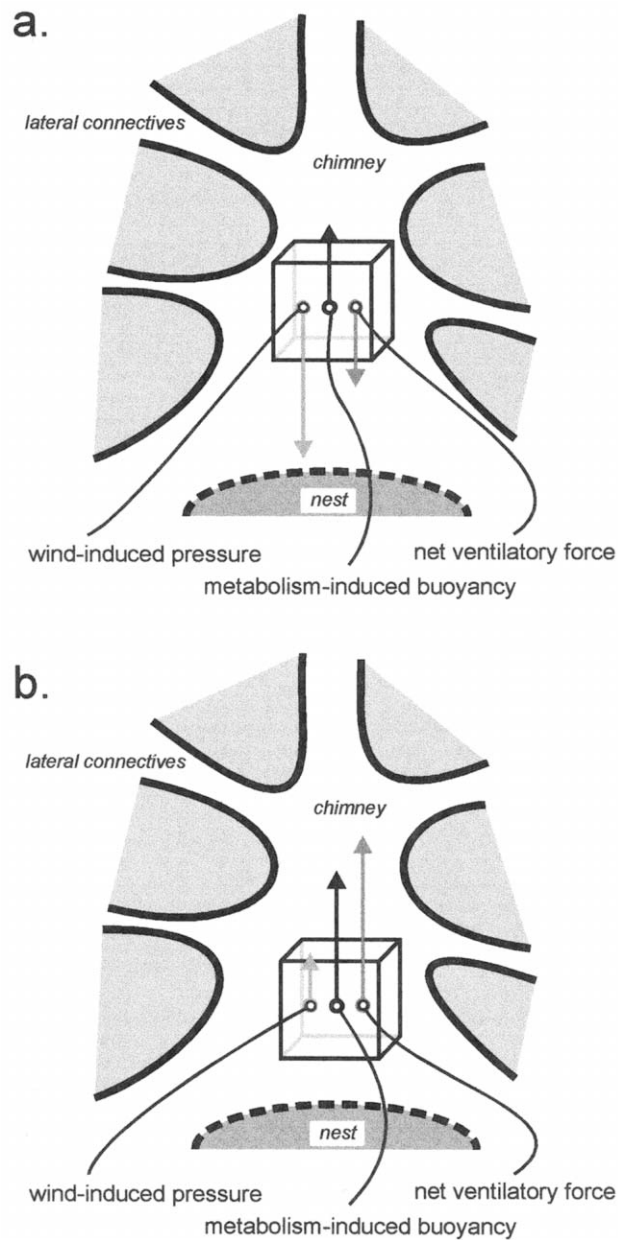
Figure 20. Pulse-chase experiment for mound 44 on January 10, 1998. Sensors were placed at several localities indicated by the filled circles on the cartoons accompanying each trace. Tracer was injected into the middle chimney. Other conventions as in Figure 8.

Figure 22. Postulated zones of gas exchange in a *Macrotermes michaelseni* mound and nest. Details in text.

Figure 21. Diagram representing balance of forces at point of equipoise posited to exist in the middle chimney. Forces on a parcel of air, represented by the cube, include metabolism-induced buoyancy, represented by an upward-pointing vector (*black*) and wind-induced pressure, represented by a vector (*light gray*) that can point either downward (*a*) or upward (*b*). The parcel moves under the influence of the resultant vector (*dark gray*), which may point either downward (*a*) or upward (*b*). As the magnitude and direction of the wind-induced pressure vector fluctuates, air in the middle chimney moves up or down in a tidal pattern.
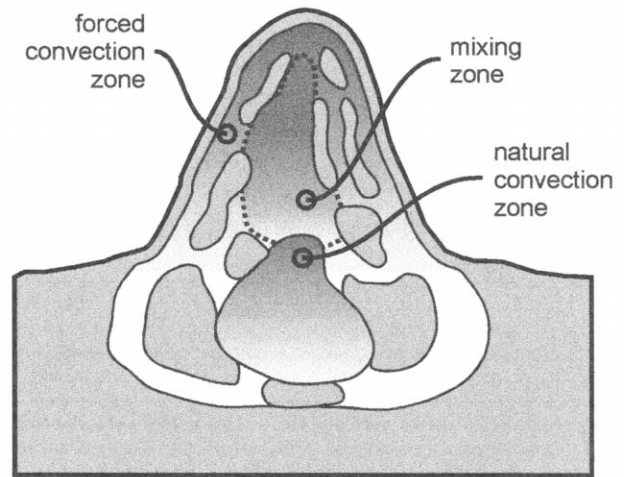
tidal, not circulatory, and are driven by temporal variation in wind speed and direction. Third, metabolism-induced natural convection is not a significant force driving bulk flows in the mound. It may, however, play a significant role in the mechanisms that underlie homeostasis of the nest's atmosphere. Taken together, these conclusions point to a substantially different picture of ventilation and respiratory gas exchange in the complex nests of macrotermitines than the thermosiphon model posited by Martin Lüscher (1961) for *Macrotermes natalensis* (*bellicosus*). This new perspective may illuminate important questions on the mechanisms and evolution of social physiology, both in the termites and in other social insects.

Air flows under the influence of a balance of forces. The thermosiphon model assumes that metabolism-induced buoyancy is the most significant force driving bulk flows of air in the mound and nest. Implicit in this assumption is that air in the mound is shielded from external sources of potential energy that could also drive flow, which include thermal energy in sunlight (Korb and Linsenmair 2000) and kinetic energy in wind. The enclosed mounds built by *M. michaelseni* and *M. natalensis* would seem to provide such an effective shield. Nevertheless, wind strongly drives movements of air in the mounds of *M. michaelseni*.

Wind exerts its strongest effect on the mound's network of surface conduits. Wind imposes a complex field of pressure over the mound's surface (Figs. 9–11), and this is imparted to air in the surface conduits through their porous walls. These pressures drive substantial bulk movements of air within the surface conduits. Tracer injected into a surface conduit, whether the point of injection be upwind or downwind, rapidly accumulates in downwind and flanking surface conduits, particularly high on the mound surface where suction pressures are
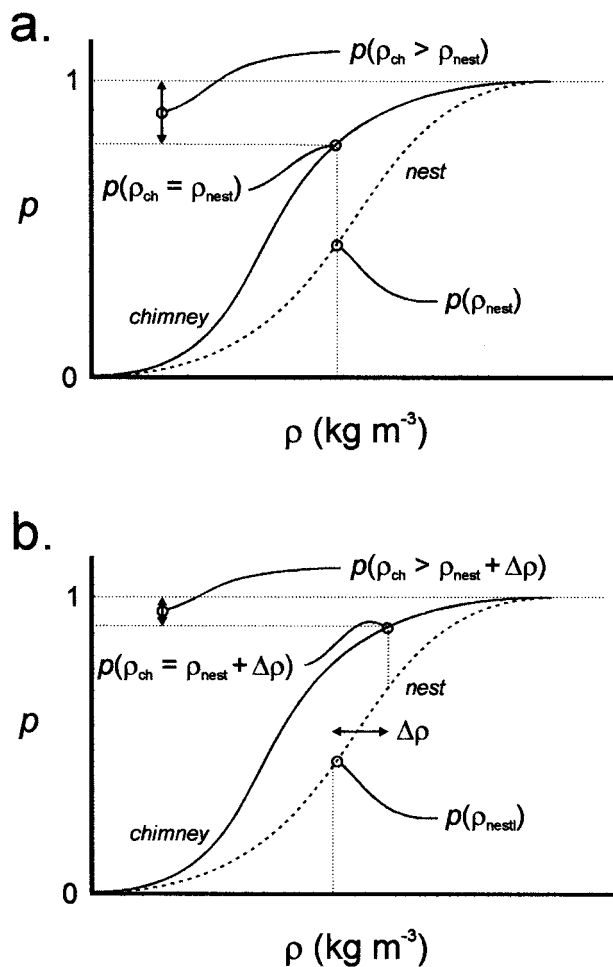
Figure 23. Estimation of probabilities of density gradients in the mound and nest. *a*, Estimate of probability that density of nest air (ρ_{nest}) is less than density of chimney air, ρ_{ch} ($\rho_{ch} > \rho_{nest}$). Cumulative probabilities (P) of particular densities are estimated from the mean and variance of estimated densities at each location. The probability that both nest air and chimney air have equal densities is the product of $P(\rho_{nest})$ and $P(\rho_{ch} = \rho_{nest})$. The probability that chimney air is denser than nest air is the product of $P(\rho_{nest})$ and $P(\rho_{ch} < \rho_{nest})$. *b*, Estimate of probability that density of chimney air is at least some quantity $\Delta\rho$ greater than nest air.

strongest (Figs. 8, 9, 12, 13). Air in the surface conduits is also vigorously mixed when wind shifts direction, "sloshing" air from one side of the mound to another (Fig. 9). Thus, the surface conduits form at least one well-mixed air space that underlies the entire mound surface.

The thermosiphon model predicts that air should circulate through the mound and nest in the following sequence: nest→ chimney → surface conduits → nest. Movements of air measured with tracers are only partly consistent with this pattern. Tracer injected into the nest appears in the chimney within

about 5 min (Fig. 17) and at the surface conduits only after 20–30 min (Fig. 13). Similarly, tracer injected into the chimney appears in the surface conduits within about 10 min (Fig. 14). However, tracer injected directly into a surface conduit does not return to the nest as would be expected in a thermosiphon flow (Fig. 16). These results are consistent with the alternative sequence: nest → chimney → lateral connectives → surface conduits, with no return path to the nest.

The thermosiphon model treats the chimney as a conduit for bulk transmission of spent nest air to the surface tunnels, where most of the exchanges of heat and respiratory gases occur. In contrast, the chimney of the *M. michaelseni* mound is an important venue for respiratory gas exchange. If the chimney were simply a conduit, humidity, Po_2, and concentrations of endogenous combustible gas would be similar in the nest and everywhere within the chimney. They are not; Po_2 and humidity decline up the chimney, indicating exchange between nest air and fresh air along the chimney's length (Fig. 5). Curiously, the decline in concentration of endogenous combustible gas, probably methane, is steeper than that for Po_2, suggesting an additional consumption of methane by methane-oxidizing bacteria (Seiler et al. 1984; Khalil et al. 1990). Finally, if the chimney simply conveyed spent nest air upward, there should be little or no exchange from the chimney back to the nest. Although
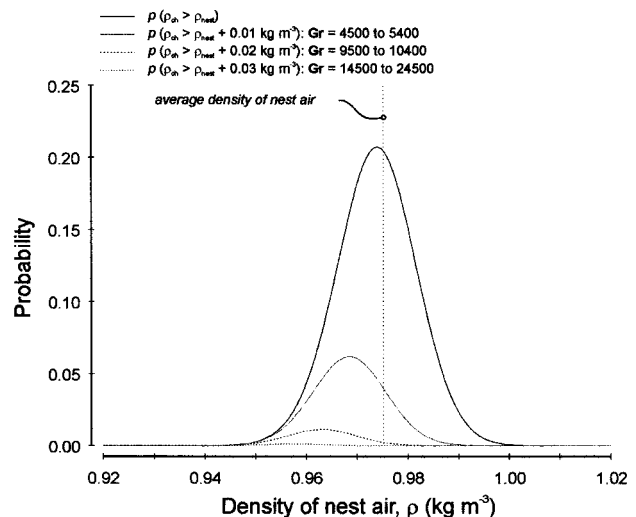

Figure 24. Estimates of the likelihood of density gradients in the mound and nest. Four scenarios are presented that describe buoyant forces that will loft air upward from the nest into the chimney. The first scenario is that there will be any upwardly directed density difference ($\rho_{ch} > \rho_{nest}$). The second is that there will be a 10-g m^{-3} density difference ($\rho_{ch} > \rho_{nest} + 0.01$ kg m^{-3}). The third is that there will be a 20-g m^{-3} density difference ($\rho_{ch} > \rho_{nest} + 0.02$ kg m^{-3}). The fourth is that there will be a 30-g m^{-3} density difference ($\rho_{ch} > \rho_{nest} + 0.03$ kg m^{-3}). Vertical dotted line represents the average density of air in the nest. Grashof numbers are estimated as described in text.
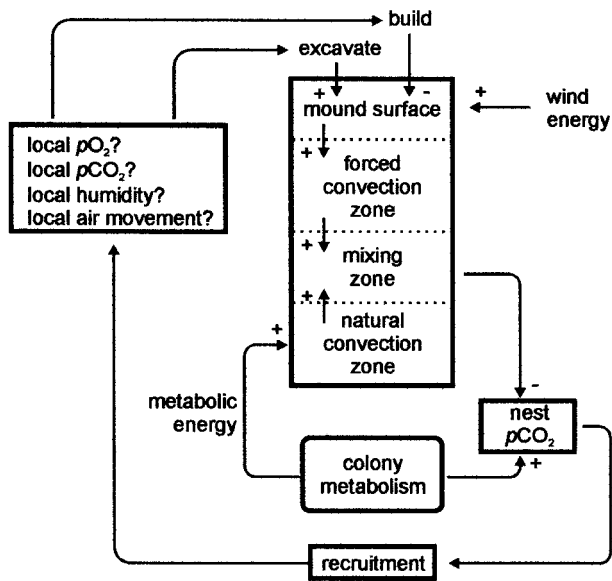
Figure 25. Posited scheme of social homeostasis in the colonies of *Macrotermes michaelseni*. Details in text. After Turner (2000*b*).

movement of tracer from chimney to nest was slight, it did occur, particularly under windy conditions (Figs. 18, 20). When it did, tracer injected into the chimney appeared in the nest and surface conduits simultaneously (Figs. 19, 20).

The exchange of gas between the chimney and surface conduits is probably mediated by the network of lateral connectives between them. Tracer injected into the chimney migrates directly to the surface conduits and vice versa (Figs. 14, 15) but with some interesting complications. First, there appears to be a hysteresis, with air moving more readily from the chimney to the surface conduits than in the reverse (Figs. 14, 15). Second, air appears to be distributed uniformly from the chimney to the surface conduits without respect to wind direction. Tracer injected into the chimney commonly appears at both upwind and downwind surfaces simultaneously. Only then does wind distribute tracer to the downwind and flanking surface conduits (Figs. 14, 20). These biases in flow are likely mediated by an interaction between metabolism-induced buoyant pressures in the chimney and wind-induced pressures in the surface conduits. The lateral connectives appear to form a damping network so that large fluctuations of pressure in the surface conduits are damped close to the chimney. Airflows close to the chimney would therefore be dominated by metabolism-induced buoyant forces, which would bias air movements uniformly outward. Closer to the surface, wind-induced pressures would come to predominate, distributing air according to their distribution over the mound surface. In this scheme, the absence of large surface vents, such as those found in other macrotermitines like *Macrotermes subhyalinus* (Weir 1973) or *Odonto-*

termes transvaalensis (Turner 1994), matters little to the mechanisms of ventilation; the interaction of the mound with wind is governed by the damping network of tunnels deep in the mound rather than by the details of the mound's surface features. Indeed, it seems likely that a common mechanism operates to ventilate macrotermitine nests that vary widely in mound architecture. This is contrary to prevailing opinion, which asserts that thermosiphon circulation will be common in enclosed nests (Lüscher 1961), while unidirectional induced flows will be common in nests with chimneys or large open vents on their mounds (Weir 1973; Darlington et al. 1997). In fact, the patterns of air movement in the nests of *M. michaelseni* are neither circulatory nor unidirectional but tidal. This is remarkably similar to the patterns of airflow seen in nests of *O. transvaalensis*, which build mounds with large open chimneys (Turner 1994).

Tidal ventilation in *M. michaelseni* nests relies on temporal variation in the speed and direction of wind. A few comments on the nature of flow and wind will be helpful here. Any fluid flow can be represented by a velocity vector, which can in turn be resolved from three mutually perpendicular component vectors. For laminar-steady flow, only one of the component vectors predominates, the one parallel to the pressure gradient that drives the flow. Turbulent flow, however, is marked by large variations in all the component vectors. A mound exposed to turbulent winds will be subject not only to forces parallel to the prevailing wind but also to substantial forces vertical to and perpendicular to the prevailing wind. Thus, as winds freshen and become more turbulent, the pressure field around the mound both strengthens and becomes more chaotic. This will induce mixing of air in the surface conduits that varies as winds alternately freshen and die.

Local weather conditions also play a role. When prevailing winds are driven by persistent cells of high or low barometric pressure, both wind speed and wind direction are turbulent, with a large steady component of flow. Winds also arise from local convective disturbances, particularly in tropical savannas where ground heating during the day is intense. Such winds are gusty, exhibiting substantial shifts of direction and speed, with substantial updraft or downdraft components (Rosenberg 1974; Campbell 1977). On the Namatubis study site, such convective disturbances are common, particularly in summer.

Tidal ventilation in the mound results from an interaction between these complex temporal variations in wind and the relatively steady buoyant forces arising from colony metabolism. Metabolism-induced buoyancy provides a slight upward bias to the movement of air into the chimney. There, spent nest air is mixed with relatively fresh air from the surface conduits. As wind speed varies, so too will the vigor of the mixing and hence the rate of gas exchange. This is shown by the effect of gusty winds on clearance of tracer gas from the chimney (Fig. 18); when winds freshen, the clearance of tracer from the chimney speeds up, while during a lull, clearance is slower.

Mixing is further enhanced by the very strong influence of wind on bulk flows in the surface conduits, most dramatically the "sloshing" movements of air induced by shifts of wind direction (Fig. 9). Such shifts are common with winds arising from convective disturbances. Tidal ventilation results when turbulent winds either enhance or oppose the upward bias arising from metabolism-induced buoyant forces (Fig. 21). Most commonly, winds will induce strong suction pressures at the mound's upper surfaces, and this will enhance the upward movement of air from the nest into the chimney. With changes of wind speed and wind direction, a tidal ventilation will result similar to that seen when honeybees fan synchronously in place at the entrance of an overheated hive (Southwick and Moritz 1987; Turner 2000b). The overall effect is reminiscent of gas exchange in the lung but with wind rather than muscles providing the motive power. As in the lung, gas exchange occurs under the influence of three regimes: a forced convection zone (that encompasses the surface conduits), a zone dominated by metabolism-induced natural convection, and a mixing zone encompassing the middle chimney (Fig. 22).

Tidal ventilation in the mound requires there to be in the chimney an equipoise between wind-induced pressures and metabolism-induced buoyant forces. Several lines of evidence point to such an equipoise. First, metabolism-induced buoyant forces are likely to be weak; indeed, the distribution of average air densities in the nest and mound do not favor buoyant forces at all (Table 5). Consequently, buoyancy seems equally likely to stratification of air in the chimney. Conditions that should favor strong buoyant forces in the chimney are possible, but they will be rare. Temperature is the largest component of variation in estimated air density. Temperatures that differ much from the average may promote natural convection or may promote stability. The likelihood for such conditions could be, in principle, derived from the mean and variance of temperatures throughout the mound and nest (Fig. 23). Although there is a substantial probability that nest air will be lighter to any degree than air in the middle chimney (Korb and Linsenmair 2000), the probability that the density difference will be large enough to actually drive a bulk flow is considerably less. For example, the probability of a density difference of 0.01 kg m^{-3} is at best 6% (Fig. 24). The probability of larger density differences is smaller still; for a minimum density difference of 0.02 kg m^{-3}, the probability is around 1% (Fig. 22). This corresponds to a Grashof number of around 10,000, which is substantially less than Grashof numbers that correspond to most natural convection flows, which range from roughly 10^5 to 10^7. A similar analysis can be performed for temperature variations that promote stability, but the outcome is similar; rarely will such conditions occur.

Thus, buoyant pressures in the chimney most likely hover at around a few pascals above or below prevailing pressure. It is noteworthy that these pressures are similar in magnitude to the wind-induced pressures observed in the surface conduits, which averaged about an 8-Pa m^{-1} difference from top of the mound to its bottom and ranged from 1 to 25 Pa m^{-1} (Fig. 7). If these pressures were damped by the network of lateral connectives between the chimney and surface conduits, wind-induced chimney pressures should hover at around about the same level as the metabolism-induced buoyant forces: equipoise.

Clearance of tracer from different localities in the mound and nest is suggestive of such an equipoise (Table 3). Tracer clears rapidly from the upper parts of the chimney, probably due to the vigorous action of winds high off the ground. Similarly, tracer clears rapidly from the nest into the chimney, driven there probably by metabolism-induced buoyancy. In the middle chimney, however, the air is relatively stagnant, requiring roughly twice as long to clear as it does from the upper chimney and nest (Table 3). This stagnation could result from a balance between wind-induced pressures from above and metabolism-induced pressures from below. Finally, there is a weak tidal movement of tracer between chimney and nest in synchrony with winds (Figs. 17–19), also suggestive of an equipoise in the middle chimney.

These results shed new light on the phenomenon of social homeostasis in termite colonies. Homeostasis is a regulatory process that matches a physiologically driven flux of matter or energy against some physically driven flux of the same (Turner 2000b). For example, a steady concentration of CO_2 in the nest atmosphere of a termite nest results when the colony's production rate of CO_2 (a physiological flux) is matched to the flux rate of CO_2 across the walls of the surface conduits (a physical flux). In a M. michaelseni mound, homeostasis of the nest atmosphere could result from a simple adjustment of mound height. Boundary layer wind speeds on-site varied substantially with height (Table 4). Ventilation rate could therefore be adjusted through adjustments in the height of the mound; taller mounds would capture more wind energy and be more vigorously ventilated than would shorter mounds. Social homeostasis would result from adaptive modification of mound height so that the capture of wind energy was matched to the respiratory gas flux of the colony. The key to social homeostasis is in how the members of the colony assess whether the mound is at the "right" height.

The equipoise of pressures in the middle chimney could provide the termites with a gauge for indirectly assessing mound height. An equipoise in the middle chimney is, by definition, the point at which wind energy for ventilation is equal to the colony's metabolism-induced buoyant forces. If these are out of balance, one of two states will occur. If the capture of wind energy is insufficient, metabolism-induced natural convection will dominate movements of air in the nest. The likely result would be an elevation of carbon dioxide concentration, humidity, methane, and volatile chemicals throughout the mound. However, if the mound is capturing more wind energy than is needed to match colony respiratory flux, the opposite trends will

ensue. Additionally, wind-driven bulk flows of air ("breezes") will increase throughout the mound and may even extend into the nest itself. Termites are exquisitely sensitive to changes of local P_{CO_2}, P_{O_2}, humidity, and slight breezes (Nicolas and Sillans 1989) and will respond by altering the local structure (Stuart 1972), opening holes in the mound surface if things get too stuffy, and plugging holes in response to local breezes, low P_{CO_2}, and other stimuli (Fig. 25).

Therefore, social homeostasis in a *M. michaelseni* colony is, at root, a problem of mound morphogenesis. If mechanisms of mound morphogenesis can be tied to functional stimuli that initiate these mechanisms, homeostasis should emerge more or less spontaneously from the assemblage. For example, Turner (2000*a*) has proposed a simple model for morphogenesis of *M. michaelseni* mounds in which most of the mound's architectural features are explainable by subtle biases in the translocation of soil by worker termites. The hypothetical biases arise from workers acting as conveyors of soil along gradients of P_{CO_2}, with intensity of soil translocation correlated to the steepness of the gradient. Thus, mound remodeling should be most intense in those areas where gradients in P_{CO_2} are the steepest. Homeostasis results because the resultant remodeling also changes the gradients in P_{CO_2} that initiate remodeling in the first place. Thus, mound architecture is part of a feedback loop in which architecture is both cause and effect of the P_{CO_2} gradients within the mound. Homeostasis will evolve through natural selection acting on the coupling functions that link distribution of P_{CO_2} with soil translocation. This model, which regards mound architecture as a process rather than as a superorganismal analogue of phenotype, is a new way of looking at the evolution of social homeostasis in the complex nests of the advanced termites.

Acknowledgments

Literature Cited

Abe T. and J.P.E.C. Darlington. 1985. Distribution and abundance of a mound-building termite, *Macrotermes michaelseni*, with special reference to its subterranean colonies and ant predators. Physiol Ecol Jpn 22:59–74.

Batra L.R. and S.W.T. Batra. 1979. Termite-fungus mutualism. Pp. 117–163 in L.R. Batra, ed. Insect-Fungus Symbiosis: Nutrition, Mutualism and Commensalism. Wiley, New York.

Campbell G.S. 1977. An Introduction to Environmental Biophysics. Springer, New York.

Coaton W.G.H. and J.L. Sheasby. 1972. Preliminary report on a survey of the termites (Isoptera) of south West Africa. Cimbebasia Mem 2:1–129.

Collins N.M. 1979. The nests of *Macrotermes bellicosus* (Smeathman) from Mokwa, Nigeria. Insectes Soc 26:240–246.

Darlington J.P.E.C. 1984. Two types of mounds built by the termite *Macrotermes subhyalinus* in Kenya. Insect Sci Appl 5:481–492.

———. 1985. The structure of mature mounds of the termite *Macrotermes michaelseni* in Kenya. Insect Sci Appl 6:149–156.

Darlington J.P.E.C., P.R. Zimmerman, J. Greenberg, C. Westberg, and P. Bakwin. 1997. Production of metabolic gases by nests of the termite *Macrotermes jeaneli* in Kenya. J Trop Ecol 13:491–510.

Garnier-Sillam E., F. Toutain, and J. Renoux. 1988. Comparaison de l'influence de deux termitiéres (humivore et champignonniste) sur las stabilité structurale des sols forestiers tropicaux. Pedobiologia 32:89–97.

Grassé P.P. and C. Noirot. 1961. Nouvelles recherches sur la systématique et l'éthologie des termites champignonnistes du genre *Bellicositermes* Emerson. Insectes Soc 8:311–359.

Harris W.V. 1956. Termite mound building. Insectes Soc 3:261–268.

Kalshoven L.G.E. 1956. Observations on the inner structure of *Macrotermes gilvus* mounds in Java. Insectes Soc 3:269–272.

Khalil M.A.K., R.A. Rasmussen, J.R.J. French, and J.A. Holt. 1990. The influence of termites on atmospheric trace gases.

CH_4, CO_2, $CHCl_3$, N_2O, CO, H_2, and light hydrocarbons. J Geophys Res 95D4:3619–3634.

Korb J. and K.E. Linsenmair. 2000. Ventilation of termite mounds: new results require a new model. Behav Ecol 11:486–494.

Loos R. 1964. A sensitive anemometer and its use for the measurement of air currents in the nests of *Macrotermes natalensis* (Haviland). Pp. 364–372 in A. Bouillon, ed. Etudes sur les termites africains. Maisson et Cie, Paris.

Lüscher M. 1956. Die Lufterneuerung im nest der termite *Macrotermes natalensis* (Haviland). Insectes Soc 3:273–276.

———. 1961. Air conditioned termite nests. Sci Am 238:138–145.

Nicolas G. and D. Sillans. 1989. Immediate and latent effects of carbon dioxide on insects. Annu Rev Entomol 34:97–116.

Peakin G.J. and G. Josens. 1978. Respiration and energy flow. Pp. 111–163 in M.V. Brian, ed. Production Ecology of Ants and Termites. Cambridge University Press, Cambridge.

Pomeroy D.E. 1977. The distribution and abundance of large termite mounds in Uganda. J Appl Ecol 14:465–475.

Rosenberg N.J. 1974. Microclimate: The Biological Environment. Wiley, New York.

Rouland C., F. Lenoir, and M. LePage. 1991. The role of symbiotic fungus in the digestive metabolism of several species of fungus-growing termites. Comp Biochem Physiol 99A:657–663.

Ruelle J., W. Coaton, and J. Sheasby. 1975. National survey of the Isoptera of southern Africa eight: the genus Macrotermes Holmgren (Termitidae: Macrotermitinae). Cimbebasia 3A:73–94.

Ruelle J.E. 1964. L'architecture du nid de *Macrotermes natalensis* et son sens fonctionnel. Pp. 327–362 in A. Bouillon, ed. Etudes sur les termites africains. Maisson et Cie, Paris.

———. 1970. A revision of the termites of the genus *Macrotermes* from the Ethiopian region (Isoptera: Termitidae). Bull Br Mus (Nat Hist) Entomol 24:366–444.

———. 1975. *Macrotermes michaelseni* (Sjöstedt): a new name for *Macrotermes mossambicus* (Hagen) (Isoptera: Termitidae). J Entomol Soc South Afr 40:119.

———. 1985. Order Isoptera (termites). Pp. 53–61 in C.H. Scholtz and E. Holm, eds. Insects of Southern Africa. Butterworth, Durban.

Seiler W., R. Conrad, and D. Scharffe. 1984. Field studies of methane emissions from termite nests into the atmosphere and measurement of methane uptake by tropical soils. J Atmos Chem 1:171–186.

Southwick E.E. and R.F.A. Moritz. 1987. Social control of ventilation in colonies of honey bees, *Apis mellifera*. J Insect Physiol 33:623–626.

Stuart A.M. 1972. Behavioral regulatory mechanisms in the social homeostasis of termites (Isoptera). Am Zool 12:589–594.

Tracy C., W. Welch, and W. Porter, eds. 1980. Properties of Air: A Manual for Use in Biophysical Ecology. 3d ed. University of Wisconsin Press, Madison.

Turner J.S. 1994. Ventilation and thermal constancy of a colony of a southern African termite (*Odontotermes transvaalensis*: Macrotermitinae). J Arid Environ 28:231–248.

———. 2000a. Architecture and morphogenesis in the mound of *Macrotermes michaelseni* (Sjöstedt) (Isoptera: Termitidae, Macrotermitinae) in northern Namibia. Cimbebasia 16:143–175.

———. 2000b. The Extended Organism: The Physiology of Animal-Built Structures. Harvard University Press, Cambridge, Mass.

Vogel S. 1981. Life in Moving Fluids. Willard Grant, Boston.

Weir J.S. 1973. Air flow, evaporation and mineral accumulation in mounds of *Macrotermes subhyalinus*. J Anim Ecol 42:509–520.

Wilson E.O. 1971. The Insect Societies. Harvard University Press, Cambridge, Mass.